ACADÉMIE
DES SCIENCES
INSTITUT DE FRANCE

Comptes Rendus
Physique

Bernard Castaing, Francesca Chillà, Julien Salort, Yann Fraigneau and Anne Sergent

The inertial regimes in Rayleigh–Bénard convection

Volume 26 (2025), p. 587-617

Online since: 24 September 2025

https://doi.org/10.5802/crphys.257

The Comptes Rendus. Physique *are a member of the Mersenne Center for open scientific publishing*
www.centre-mersenne.org — e-ISSN : 1878-1535

ACADÉMIE DES SCIENCES
INSTITUT DE FRANCE

Comptes Rendus. Physique
2025, Vol. 26, p. 587-617
https://doi.org/10.5802/crphys.257

Research article / *Article de recherche*

The inertial regimes in Rayleigh–Bénard convection

Les régimes inertiels de la convection de Rayleigh–Bénard

Bernard Castaing [a], Francesca Chillà [*,b], Julien Salort [b], Yann Fraigneau [c] and Anne Sergent [c]

[a] Laboratoire des écoulements géophysiques et industriels, Domaine Universitaire, CS 40700, 38058 Grenoble Cedex 9, France

[b] ENSL, CNRS, Laboratoire de physique, 69342 Lyon, France

[c] Université Paris-Saclay, CNRS, Laboratoire Interdisciplinaire des Sciences du Numérique, 91405 Orsay, France

E-mail: francesca.chilla@ens-lyon.fr

Abstract. Most theoretical studies of Rayleigh–Bénard Convection assume that the velocity boundary layer develops on the whole width or height H of the convection cell, or that the development length h scales with H. We argue that it is probably not the case, and examine the consequences of an intermediate asymptotics hypothesis in the sense of Barenblatt [1], the development length h scaling with the Nusselt number: $h \propto H\mathrm{Nu}^{-\alpha}$. This hypothesis is checked through existing experimental data, which show that α can take several different values. The analysis of Grossmann and Lohse [2] is reexamined with this new point of view, stressing on pure scaling regimes.

Résumé. La plupart des études théoriques sur la convection de Rayleigh–Bénard supposent que la couche limite de vitesse se développe sur toute la largeur ou la hauteur H de la cellule de convection, ou que la longueur de développement h est proportionnelle à H. Nous soutenons qu'il est probablement incorrect de faire cette supposition, et nous examinons les conséquences d'une hypothèse d'asymptotique intermédiaire au sens de Barenblatt [1], où la longueur de développement h dépend du nombre de Nusselt: $h \propto H\mathrm{Nu}^{-\alpha}$. Cette hypothèse est vérifiée à partir de données expérimentales existantes, qui montrent que α peut prendre plusieurs valeurs différentes. L'analyse de Grossmann et Lohse [2] est réexaminée sous cette nouvelle perspective, en mettant l'accent sur les régimes d'échelle pure.

Keywords. Hydrodynamics, Thermal Convection, Turbulence, Boundary layers, Scaling laws.

Mots-clés. Hydrodynamique, Convection thermique, Turbulence, Couches limites, Lois d'échelle.

Funding. This project was provided with computing HPC and storage resources by GENCI at CINES and TGCC thanks to the grants 2022, 2023 and 2024-2A00326 on the supercomputer Joliot Curie's ROME and Adastra's GENOA partitions.

Manuscript received 7 October 2024, revised 24 June 2025, accepted 2 July 2025.

* Corresponding author

1. Table of notations

Symbol	Definition	1st eq. of occurrence
u_i	i-component of the velocity	(1)
θ	Local temperature fluctuation	(1)
ν	Kinematic viscosity	(1)
β	Thermal expansion	(1)
κ	Heat diffusivity	(3)
g	Gravitational acceleration	(4)
H	Height of the cell	(4)
Δ	Temperature difference between plates	(4)
Ra	Rayleigh number	(4)
Pr	Prandtl number	(5)
L	Horizontal dimension of the cell	(6)
Γ	Aspect ratio	(6)
$\dot{Q}$	Vertical heat flux	(7)
C_p	Isobaric heat capacity of the fluid	(7)
Nu	Nusselt number	(7)
U	Typical velocity of the fluid	(8)
Re	Reynolds number	(8)
Θ	Typical temperature fluctuations	(9)
Ft	Relative temperature fluctuations	(9)
μ	Exponent of the Nu vs Ra relation	(10)
ε	Viscous dissipation per unit mass	(12)
ϵ_T	Thermal dissipation	(13)
χ	Vertical velocity-temperature correlation coefficient	(17)
h	Development length of the boundary layer	(19)
α	Exponent of h vs Nu dependence	(19)
δ	Size of the thermal boundary layer	(20)
γ	Horizontal velocity vertical gradient	(21)
A, K	Constants of the Ching's solution	(24)
Pe	Peclet number	(26)
λ	Size of the velocity boundary layer	(34)
L_p	Total length of the plumes on the region of measurement	(38)
S	Area of the region of measurement	(38)
$\varepsilon_{\mathrm{bl}}$	Boundary layer contribution to the viscous dissipation	(57)
v_*	Friction velocity	(62)
y_+	Reduced distance to the plate	(65)
DVB	Relative part of the bulk in the viscous dissipation	(78)
DVL_l, DVL_u	Relative part of the boundary layer in the viscous dissipation	(79)
Δ^*	Twice the temperature difference across a thermal boundary layer	(89)
σ	Thermal dissipative scale in the bulk	(94)
ϑ	Temperature fluctuation at the thermal dissipative scale	(94)
v_σ	Velocity fluctuation at the thermal dissipative scale	(95)
η	Viscous dissipative scale in the bulk	(96)
v_η	Velocity fluctuation at the viscous dissipative scale	(96)

2. Introduction

Convection is ubiquitous. Among other important problems, it governs the behavior of stars, the climate of planets, or the behavior of the molten core in a damaged nuclear plant. However, the bridge between these large scale events and their laboratory counter part, the Rayleigh–Bénard convection cell is not yet firmly set.

The Rayleigh–Bénard convection cell consists in a Newtonian, nearly incompressible, isotropic fluid, of kinematic viscosity ν, of heat diffusivity κ, of thermal expansion β, put into motion by a vertical heat flux $\dot{Q}$. The problem is generally treated within the Boussinesq approximation, whose equations write:

$$\partial_t u_i + u_j \partial_j u_i = -\frac{1}{\rho}\partial_i p + g_i \beta\theta + \nu \partial_j \partial_j u_i, \tag{1}$$

$$\partial_j u_j = 0, \tag{2}$$

$$\partial_t \theta + u_j \partial_j \theta = \kappa \partial_j \partial_j \theta, \tag{3}$$

where g_i and u_i are the i components of the gravitational acceleration and the velocity, and θ is the temperature.

The non dimensional control parameters are the Rayleigh number:

$$\mathrm{Ra} = \frac{g\beta\Delta H^3}{\nu\kappa}, \tag{4}$$

where g is the gravitational acceleration, Δ the temperature difference between the horizontal plates, the hot one (generally below) and the cold one, H the vertical distance between these plates. Of importance are also the Prandtl number:

$$\mathrm{Pr} = \frac{\nu}{\kappa}, \tag{5}$$

and the parameters specifying the shape of the cell, as the aspect ratio:

$$\Gamma = \frac{L}{H}, \tag{6}$$

where L is the typical horizontal dimension of the plates.

The non dimensional parameters measuring the response of the cell are the Nusselt number:

$$\mathrm{Nu} = \frac{\dot{Q}H}{C_p \kappa \Delta}, \tag{7}$$

where C_p is the isobaric heat capacity of the fluid per unit volume. The Reynolds number:

$$\mathrm{Re} = \frac{UH}{\nu}, \tag{8}$$

where U is a typical velocity of the fluid, and the relative temperature fluctuations:

$$\mathrm{Ft} = \frac{\Theta}{\Delta}, \tag{9}$$

where Θ is a typical temperature fluctuation in the bulk, generally depend on the way and the point where the measures of U and Θ are made, but are nevertheless precious indications of the nature of the flow.

During the second half of the past century, many propositions have been made for the Ra dependence of Nu, most of them as a power law (for a review, see [2–5]):

$$\mathrm{Nu} = \mathrm{Ra}^{\mu}, \tag{10}$$

with occasional logarithmic corrections. Absolute majoration has been derived [6], showing that, whatever the Prandtl number, in the limit of large Ra:

$$\mathrm{Nu} < C\mathrm{Ra}^{1/2}, \quad \text{where } C \text{ is a constant.} \tag{11}$$

Within approximately the same period, a great number of experiments [2–4] have been performed, including numerical experiments, reaching up to $\mathrm{Ra} = 10^{17}$, generally analyzed as power laws, equation (10), or a succession of power laws. It results in a wide variety of μ values proposed, both theoretically and experimentally.

In the past two decades, in a series of seminal papers, S. Grossmann and D. Lohse (GL) (see [7]; for the last version, see [8]) have proposed to rely the predictions to two exact results concerning the viscous (ε) and thermal (ε_T) dissipations per unit mass:

$$\varepsilon = \nu\langle\partial_i u_j \partial_i u_j\rangle = \frac{\kappa^3}{H^4}\mathrm{Ra}\,(\mathrm{Nu}-1)\,\mathrm{Pr}, \tag{12}$$

$$\varepsilon_T = \kappa\langle\partial_i T \partial_i T\rangle = \frac{\kappa\Delta^2}{H^2}\mathrm{Nu}. \tag{13}$$

As remarked by Lohse and Shishkina [5], these relations are known since long, and can be traced at least to the works of Malkus [9].

Remarking that each dissipation can be dominated either by the boundary layer or by the bulk, they proposed to classify the flows into four categories:

(I) both dissipations are dominated by the boundary layer;
(II) thermal dissipation dominated by the boundary layer, viscous by the bulk;
(III) viscous dissipation dominated by the boundary layer, thermal by the bulk;
(IV) both dissipations are dominated by the bulk.

Moreover, each category has the subscript "u" for the large Pr, and "l" for the small ones, and has a prime "′" if the boundary layer is turbulent. Evaluating the bulk and boundary layer dissipations, both viscous and thermal, and using the exact relations (12) and (13), GL could obtain the Nu and Re numbers in a wide range of intermediate values of Ra and Pr. For instance, the bulk dissipation per unit mass is often evaluated as [7,10]:

$$\varepsilon_b = \frac{U^3}{H} = \frac{U^3}{H^3}\frac{\nu^3}{\kappa^3}\frac{\kappa^3}{H^4} = \frac{\kappa^3}{H^4}\mathrm{Re}^3\mathrm{Pr}^3. \tag{14}$$

Assuming that the viscous dissipation is dominated by the bulk then gives, using equation (12):

$$\mathrm{Ra}\,(\mathrm{Nu}-1) = \mathrm{Re}^3\mathrm{Pr}^3. \tag{15}$$

Ad hoc cross-over functions, and adjustable parameters were necessary, fitted to the existing experimental data. As a result, as remarked by GL, none of the pure regimes described in the above table appears alone, the combination of two of them being undistinguishable from a pure power law as equation (10).

In this paper, we shall follow the same way, relying to the exact results (12) and (13), and evaluating the bulk and boundary layer dissipations. However, our approach will differ from the GL one on the following points:

- We shall take into account the various possible regimes, both in the bulk and in the boundary layer. We shall stress the influence of the so called mixing transition [11,12] in the bulk, and we shall reinterpret the mixing buffer zone of Kadanoff et al. [13].
- While recognizing the possibility of crossovers we shall stress on pure regimes, finding evidences of them in published experimental data.
- We renounce to the dogma of single Nu or Re values for given Ra and Pr, even at a given aspect ratio.

Indeed, such different regimes, at same Ra, Pr, and Γ numbers, have been observed not only between different experiments, as the Wu [14] and Chavanne [10] ones, but also within the same experiment [15–17]. Mechanisms have been proposed for such multi-stability [18]. We shall not treat this subject, focusing on the simple description of possible regimes.

The paper is organized as follows. In Section 3, we shall check a hypothesis made in several models, that the product of the typical velocity and the typical temperature fluctuations well represents their cross-correlation, i.e. that their cross-correlation coefficient is constant. In Section 4, we shall introduce the development length of the velocity boundary layer, and make the hypothesis of a simple scaling of this length with the Nusselt number. We shall examine how it influences the velocity and thermal boundary layers. In Section 5, we shall check the above hypothesis. In Section 6, we shall evaluate the viscous dissipation, in the boundary layer, distinguishing between Blasius or logarithmic ones, and in the bulk, distinguishing between soft and hard turbulence. This goes through a determination of the velocity boundary layer width, λ, which we use in Section 7 for determining the thermal one δ. In Section 8, we evaluate the thermal dissipation, particularly in the bulk, where we distinguish between soft and hard turbulence. In Section 9, we use all our results for discussing some remarkable cases, before to conclude in Section 10.

3. The cross-correlation between temperature and vertical velocity

We shall begin examining an assumption made by several models, the proportionality between the temperature and vertical velocity correlation $\langle u_z\theta\rangle$, and the product of the typical velocity U with the typical temperature fluctuation Θ. Noting that:

$$\mathrm{Nu} = \frac{\langle u_z\theta\rangle H}{\kappa\Delta}, \tag{16}$$

the coefficient of cross-correlation can be obtained as:

$$\chi = \frac{\langle u_z\theta\rangle}{U\Theta} = \frac{\mathrm{Nu}}{\mathrm{Re}\,\mathrm{Pr}}\frac{\Delta}{\Theta}. \tag{17}$$

Unfortunately, very few experimental or numerical work give simultaneous estimations of Nu, Re and temperature fluctuations for given Ra and Pr numbers. We had access to two of them: the PhD thesis of X. Z. Wu [14] and the work of Chavanne et al. [10]. For the latter, we used unpublished complementary materials, namely long simultaneous records of two close by thermometers, whose cross-correlation allowed to determine the Reynolds number.

Roche et al. [19], and independently Ahlers [20], realized that the influence of the walls is much larger than previously assumed. For both the above sets of data, we applied the correction proposed by Roche et al. [19] to the Nusselt values, to take into account the finite heat conductivity of the walls. For more recent data, we assumed the corrections made.

We also used data from the work of Musilova et al. [21]. We obtained an estimation of Ft (equation (9)) for these data using a fit of their results, shown on their Figure 6:

$$\mathrm{Ft}_M = \left(0.433 + 0.0125 \times \log_{10}(\mathrm{Ra})\right)\mathrm{Ra}^{-1/7}. \tag{18}$$

The data of Wu [14], Figure 1, show large variations for $\mathrm{Ra} < 10^8$, and an approximately constant value for larger Ra. We plot on the same figure the values of the local true correlation coefficient $\langle u_z\theta\rangle / \sqrt{\langle u_z^2\rangle\langle\theta^2\rangle}$ at various places for a numerical simulation of a rectangular Rayleigh–Bénard cell of dimensions 1, 0.25, 1 [22,23]. The simulation again shows two regimes, one variable, and one constant. The apparent agreement of the numerical values for the simulation and the Wu experiment is probably fortuitous, as neither the shapes of the cells, nor the Prandtl numbers are the same. The succession of regimes in the simulation is more similar to the Musilova et al. [21] one (see Figure 2). The remarkable point for the simulation is that the correlation in the center, where the fluctuations are very weak, is approximately the same as in much more active regions.

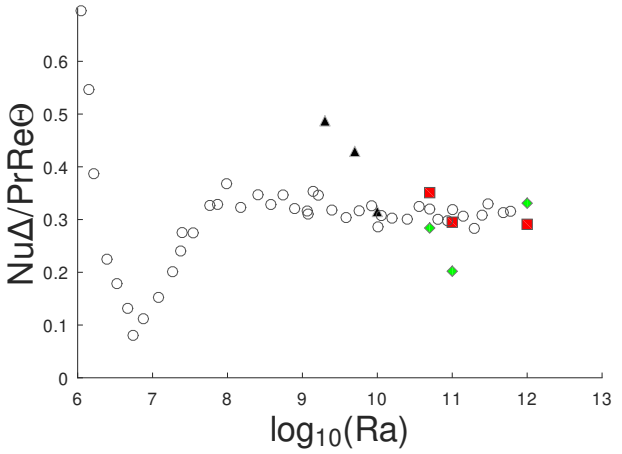

Figure 1. Open symbols: the "correlation coefficient" χ for the X. Z. Wu results [14]. Full symbols: the true correlation coefficient $\langle u_z\theta\rangle/\sqrt{\langle u_z^2\rangle\langle\theta^2\rangle}$ at various places for a numerical simulation of a rectangular Rayleigh–Bénard cell of dimensions 1, 0.25, 1 [22,23]. Black triangles: point $(0.25, 0.125, 0.5)$. Red squares: point $(0.35, 0.125, 0.5)$. Green diamonds: point $(0.5, 0.125, 0.5)$ (middle of the cell).

The data of Chavanne et al. [10], Figure 2, show two plateaus, separated by a transition in the neighborhood of $\mathrm{Ra} \simeq 3 \cdot 10^9$. The data of Musilova et al. [21] show large variations at low Ra, but are in close agreement with Chavanne et al. for $\mathrm{Ra} > 10^{10}$.

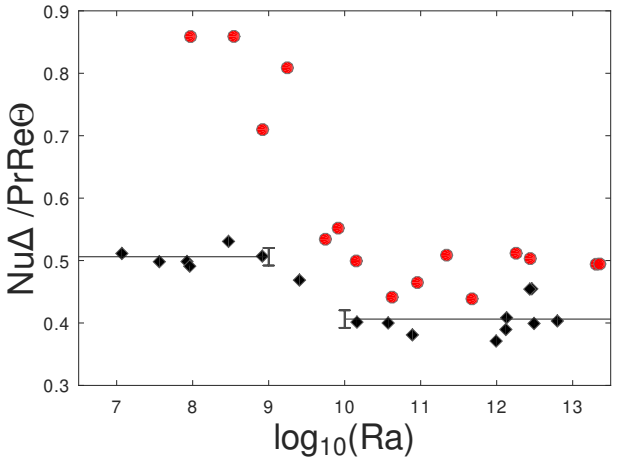

Figure 2. The correlation coefficient χ for the Chavanne et al. results [10], black diamonds, and the Musilova et al. ones [21], red circles. For the Chavanne results, we have estimated the uncertainty s_1 on the first plateau through $s_1^2 = \left(\sum_{i=1}^{6}\left(y_i - \langle y\rangle\right)^2\right)/5$ as we have 6 points. We operate similarly for the uncertainty s_2 on the second plateau, where we have 9 points. The difference between the two plateaus is five times $s = \sqrt{s_1^2 + s_2^2}$.

We thus have different cases. In some ranges, the cross-correlation coefficient between velocity and temperature cannot be considered as constant. The basic assumption made in

many models thus fails. On the other hand, however, there are ranges where the cross-correlation coefficient is constant. The usual approaches can then be used.

4. The development length. Relation between thermal and velocity boundary layers

In this section, our analysis will be at variance with most of previous ones, which consider that the velocity boundary layers develop on the whole width or height of the cell. We shall explicitly introduce the development length h as a new parameter (see Figure 3), and we shall assume that it is related to the Nusselt number as:

$$\frac{h}{H} = \mathrm{Nu}^{-\alpha}. \tag{19}$$

In all this paper, we shall renounce to precisely determine the constant factors, so our equality rather means proportionality. The above relation is inspired by the idea that the thermal boundary layer in some way governs the velocity one.

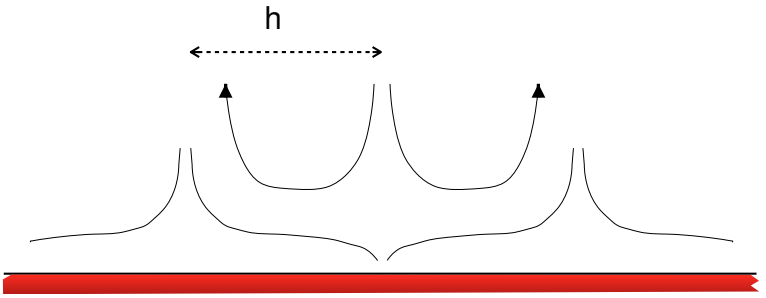

Figure 3. Sketch of a descending plume impacting the bottom plate, and two plumes rising, which shows our idea of what is the development length h.

4.1. *Large Prandtl numbers*

To our knowledge, the only work which considers the possibility of a development length which differs from H is that of E. S. C. Ching [24]. Ching solved the problem of the vertical (z) temperature profile within the velocity boundary layer, for large Prandtl number. Under some conditions, she found a self similar solution:

$$T - T_p = \Delta f\big(z/\delta(x)\big), \tag{20}$$

T_p being the temperature of the plate ($z = 0$), and x the velocity direction.

Rather than reproducing her argument, we propose to derive the typical value of δ from dimensional arguments. The x-component of the velocity has a linear profile:

$$u_x = \gamma z. \tag{21}$$

Due to the strong anisotropy of the problem, we consider the dimensions $[x]$ and $[z]$ as independent. For example, δ is of dimension $[z]$, and h is of dimension $[x]$. The basic dimensions are thus $[x]$, $[z]$ and the time $[t]$. δ depends on γ, the temperature diffusion coefficient κ, and the development length h. The dimensions are:

$$[u_x] = \frac{[x]}{[t]}, \quad [\gamma] = \frac{[x]}{[t][z]}, \quad [h] = [x], \quad [\kappa] = \frac{[z]^2}{[t]}, \quad [\delta] = [z]. \tag{22}$$

Thus, within a numerical factor:

$$\delta = \left(\frac{\kappa h}{\gamma}\right)^{1/3}. \tag{23}$$

The solution of Ching depends on two parameters, A and K, which are linked through $f(\infty) = 1/2$. For small K, A poorly depends on K, as $A = A_o(1 - BK^2)$ with B close to 1:

$$K = \delta' \simeq \frac{\delta}{h}, A = \frac{\delta(\gamma\delta^2)'}{2\kappa} \simeq \frac{\gamma\delta^3}{\kappa h}. \tag{24}$$

"$'$" means deriving versus x, which is equivalent to divide by h in our approach. We thus agree with the result of Ching, as far as K is not too large, which means h much larger than δ.

Let us now remark that the above result, equation (23), is equivalent to postulate that a peculiar Peclet number is 1 at the limit of the thermal boundary layer. Within the velocity boundary layer, we can determine the vertical velocity component u_z through the mass conservation equation (2):

$$\partial_z u_z = -\partial_x u_x = \frac{\gamma}{h} z. \tag{25}$$

Then $u_z(\delta) = \gamma\delta^2/h$ (we omit the factor 2), and:

$$Pe = \frac{u_z \delta}{\kappa} = \frac{\gamma\delta^3}{h\kappa} = 1. \tag{26}$$

As often postulated (see for instance [25]), the thermal boundary layer limit is the point where the Peclet number is 1. But we must remember that the velocity which enters this Peclet number is the vertical velocity.

A similar idea can be applied to the velocity boundary layer λ. At $z = \lambda$, u_x reaches its main flow value. Using equation (21):

$$\lambda = \frac{U}{\gamma}. \tag{27}$$

But, for a Blasius boundary layer, λ is also the diffusion length of momentum during a time h/U:

$$\lambda = \sqrt{\frac{\nu h}{U}}. \tag{28}$$

Using now equation (25):

$$\frac{u_z(\lambda)\lambda}{\nu} = \frac{U\lambda^2}{h\nu} = 1. \tag{29}$$

The Reynolds number based on the vertical velocity is 1 at $z = \lambda$. The velocity boundary layer is the point where the momentum convective transport exceeds the diffusive one. The previous equation can also write:

$$\frac{\gamma\lambda^3}{h\nu} = \frac{\lambda^3}{\mathrm{Pr}\delta^3} = 1, \tag{30}$$

which gives the well known [26] relation between λ and δ for large Prandtl numbers, and Blasius boundary layers:

$$\lambda = \delta \mathrm{Pr}^{1/3}. \tag{31}$$

4.2. *Low Prandtl numbers*

We can apply the above ideas to the case of small Prandtl numbers, where the thermal boundary layer extends out of the velocity one. Then, equation (25) writes:

$$\partial_z u_z = -\partial_x u_x = \frac{U}{h}, \tag{32}$$

which gives $u_z(\delta) = U\delta/h$, and:

$$\mathrm{Pe} = \frac{u_z \delta}{\kappa} = \frac{U\delta^2}{h\kappa} = 1. \tag{33}$$

At the velocity boundary layer limit, λ, we rather have $U\lambda^2/h\nu = 1$. The consequence is that

$$\lambda = \delta \mathrm{Pr}^{1/2}, \tag{34}$$

giving the relation between λ and δ for small Prandtl numbers, and Blasius boundary layers.

4.3. *The transition between large and low Prandtl numbers*

The results of Ching allow to precisely determine the boundary between low and large Prandtl numbers. According to the Landau–Lifchitz textbook [26], within the Blasius model, the velocity gradient at the boundary is:

$$\gamma \simeq 0.332\sqrt{U^3/\nu x} = U/\lambda. \tag{35}$$

Then, using equation (24):

$$2A\kappa = \delta(\gamma\delta^2)' = -\gamma'\delta^3 = \frac{\nu}{0.332^2}\left(\frac{\delta}{\lambda}\right)^3. \tag{36}$$

In the small K limit (where $h \gg \delta$), Ching obtains $A \simeq 2.136$:

$$\left(\frac{\delta}{\lambda}\right)^3 = \frac{2A(0.332)^2}{\mathrm{Pr}}. \tag{37}$$

The extrapolation to $\delta = \lambda$ gives $\mathrm{Pr} \simeq 0.471$ slightly larger than the estimation by Cioni et al. [15] ($\mathrm{Pr} \simeq 0.2$) or Verzicco et al. [27] ($\mathrm{Pr} \simeq 0.3$).

5. A direct access to the development length

5.1. *By direct observation*

As many others, Puthenveettil et al. [28] remarked that plumes generally detach from the plates as vertical sheets, thus appearing as lines in the plates observations. Indeed, these plumes and the corresponding lines can be observed by anyone looking at a cup of tea. Nice visualisation of them can be seen in Zocchi et al. [29]. But Puthenveettil et al. [28] were the only ones, to our knowledge, to measure the length of these lines on a wide range of Ra and Pr. We agree with them that it is the thin "local natural convection boundary layers" around the plumes "whose thickness essentially decides the heat flux in turbulent convection". We thus shall assimilate the mean distance between the plumes with the development length h.

As Puthenveettil et al. [28] remark, this mean distance is related to the total line length L_p they measured and the area S on which the measure is made through:

$$h = \frac{S}{L_p}. \tag{38}$$

We can thus check the relation (19), looking at $L_p H/S$ versus Nu. It is shown on Figure 4. Except for the two smallest Nu values, the results nicely align as a power law. A linear regression on the data gives $\alpha \simeq 0.76$.[1]

[1] In their paper [28], Puthenveettil et al. postulate that the Rayleigh number based on the distance between plumes, $\mathrm{Ra}\,(h/H)^3$, only depends on Pr. They write it $\mathrm{Ra}^{1/3}h/H \propto \mathrm{Pr}^n$. Using equations (19), (40), and (58), it gives $\alpha = 0.8$ (very close to the 0.76 found above) and $n = 1/9$, close to the 0.1 they find.

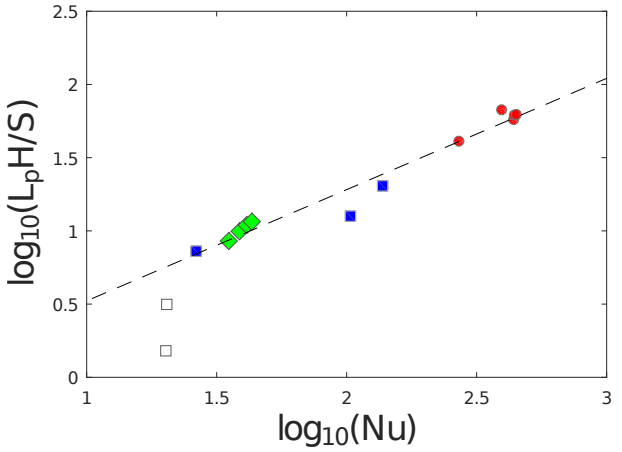

Figure 4. $L_p H/S = H/h$ (see equation (38)), where h is the development length of the boundary layer for the Puthenveettil et al. results [28], versus the Nusselt number, in a logarithmic plot. It verifies equation (19) on a large range, with $\alpha \simeq 0.76$. Diamonds: Pr = 0.7; squares: Pr = 6; circles: Pr = 602.

5.2. *Through simultaneous* Nu *and* Re *measurements*

Equations (26), (33), can be written in a different way, if the thermal dissipation is dominated by the boundary layer, thus in the GL cases (I) and (II). Then $\mathrm{Nu} = H/\delta$ (we omit the constant factor 2), and, for $\mathrm{Pr} < 1$:

$$\frac{U\delta^2}{h\kappa} = \frac{UH}{\kappa}\frac{1}{\mathrm{Nu}^2}\frac{H}{h} = 1, \quad \frac{H}{h} = \frac{\mathrm{Nu}^2}{\mathrm{Re}\,\mathrm{Pr}}, \tag{39}$$

while, for $\mathrm{Pr} > 1$, as $\gamma = U/\lambda$ and $\lambda/\delta = \mathrm{Pr}^{1/3}$:

$$\frac{\gamma\delta^3}{h\kappa} = \frac{\delta UH}{\lambda\kappa}\frac{1}{\mathrm{Nu}^2}\frac{H}{h} = 1, \quad \frac{H}{h} = \frac{\mathrm{Nu}^2}{\mathrm{Re}\,\mathrm{Pr}^{2/3}}. \tag{40}$$

Equations (39), (40), give direct access to the behavior of h, independent of our assumption, equation (19). Figures 5 and 6 show how they apply to the results of respectively X. Z. Wu, Chavanne et al. and Musilova et al. The former show a power law dependence of H/h versus Nu, on a large final range, in agreement with the postulated equation (19). A least squares regression for $\ln(\mathrm{Nu}) > 3.3$ gives $\alpha \simeq 0.48$. The Chavanne et al. results show a transition between two such laws. A least squares regression for the lowest Nusselts gives $\alpha \simeq 0.30$. A least squares regression for $\ln(\mathrm{Nu}) > 6$ gives $\alpha \simeq 0.77$, in agreement with the largest Nu values of the Musilova et al. results. The interest in Chavanne et al. set of data is the large span of Prandtl number values, which shows that no additional dependence with Pr exists out of the power law versus Nu.

As noted above, the temperature-velocity correlation coefficient χ can be considered as constant, at least within a given regime. In the expressions of H/h, it allows to replace $\mathrm{Nu}/\mathrm{Re}\,\mathrm{Pr}$ by Θ/Δ. Namely, for small Prandtl numbers:

$$\frac{H}{h} = \mathrm{Nu}\frac{\Theta}{\Delta}, \tag{41}$$

while, for large Prandtl numbers:

$$\frac{H}{h} = \mathrm{Nu}\,\mathrm{Pr}^{1/3}\frac{\Theta}{\Delta}. \tag{42}$$

When the thermal dissipation is dominated by the boundary layer (cases (I) and (II) of GL), equations (41) and (42) have potentially another interpretation. Letting aside the Prandtl dependence, it can be written: $\delta\Delta = h\Theta$, as if the heat content of the thermal boundary layer would mix in a

buffer layer of width h. This is close to the model proposed by Kadanoff et al. [13]. However, the Prandtl number dependence is hard to justify in this way.

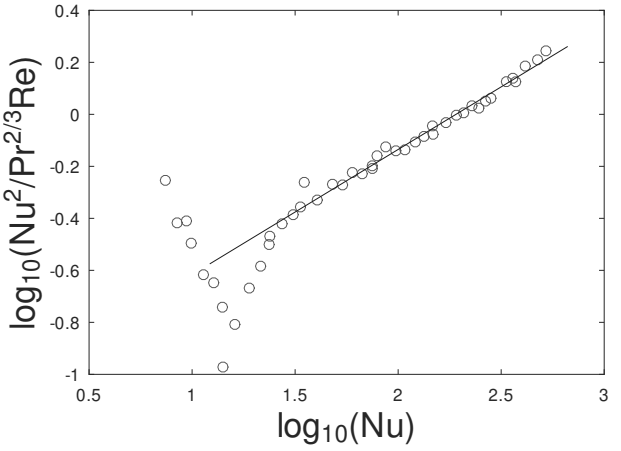

Figure 5. $\mathrm{Nu}^2/(\mathrm{Re}\,\mathrm{Pr}^{2/3}) = H/h$, where h is the development length of the boundary layer for the X. Z. Wu results [14], versus the Nusselt number, in a logarithmic plot. It verifies equation (19) on a large range, with $\alpha \simeq 0.48$.

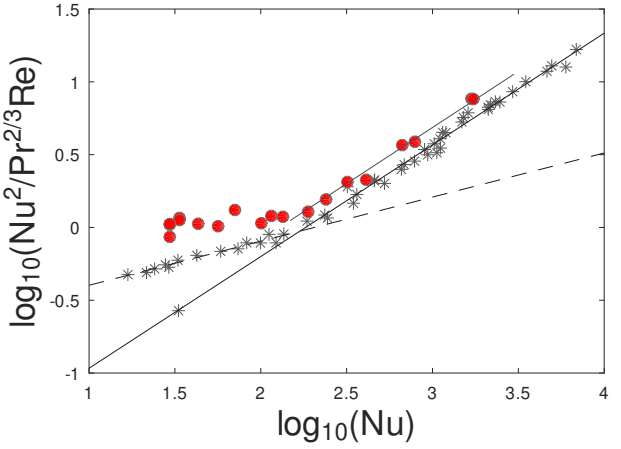

Figure 6. $\mathrm{Nu}^2/(\mathrm{Re}\,\mathrm{Pr}^{2/3}) = H/h$, where h is the development length of the boundary layer for the Chavanne et al. results [10], asterisks, and the Musilova et al. ones [21], red circles, versus the Nusselt number, in a logarithmic plot. For Chavanne et al., we have two regimes verifying equation (19), with respective slopes $\alpha \simeq 0.30$ and $\alpha \simeq 0.77$. The final regime of Musilova et al. is similar to the Chavanne et al. one.

5.3. *The α-spectrum*

We thus have an experimental confirmation of the conjecture made, equation (19), but no explanation. Up to this point, the exponent α has been an adjustable parameter. In this section we shall attempt to determine what are the possible α values, that is the α spectrum.

Indeed, the arguments presented by Kadanoff et al. [13] suggest that α should be equal to 0.5. The following discussion mainly reproduce these arguments, which have been extended to low Prandtl numbers by Cioni et al. [15].

The simplest interpretation of the development length h, is that it represents the mean distance between plumes. Let us assume with Kadanoff et al. that sheet-like plumes, of thickness λ develop. Within such a plume, the two last terms of the Navier–Stokes equation (1) should equilibrate. For small Prandtl numbers, this gives:

$$g\beta\Delta = \nu\frac{U}{\lambda^2}. \tag{43}$$

This is equivalent to write that the buoyancy force $g\beta\Delta\lambda$, corresponding to the heat content $\Delta\lambda$, equilibrates with the viscous force $\nu U/\lambda$. Equation (43) gives:

$$\frac{g\beta\Delta H^3}{\nu\kappa} = \mathrm{Ra} = \frac{\nu}{\kappa}\frac{UH}{\nu}\frac{H^2}{\lambda^2} = \mathrm{ReNu}^2, \tag{44}$$

where we used the relation (34) between λ and δ for $\mathrm{Pr} < 1$. Assuming that the bulk dominates the viscous dissipation (see equation (15)) and assimilating Nu and (Nu − 1):

$$\mathrm{Ra\,Nu} = \mathrm{ReNu}^3 = \mathrm{Re}^3\mathrm{Pr}^2. \tag{45}$$

Using equation (39):

$$\mathrm{Nu}^3 = \mathrm{Re}^2\mathrm{Pr}^2 = \mathrm{Nu}^{4-2\alpha} \tag{46}$$

and $\alpha = 0.5$.

The argument differs somewhat for $\mathrm{Pr} > 1$. Then, $\delta < \lambda$, and the heat content of the plume, of thickness λ, is only $\Delta\delta$. Equation (43) becomes:

$$g\beta\Delta\delta = \nu\frac{U}{\lambda}. \tag{47}$$

Then:

$$\frac{g\beta\Delta H^3}{\nu\kappa} = \mathrm{Ra} = \frac{\nu}{\kappa}\frac{UH}{\nu}\frac{H}{\lambda}\frac{H}{\delta} = \mathrm{Pr}^{2/3}\mathrm{ReNu}^2, \tag{48}$$

where we used the relation (31) between λ and δ for $\mathrm{Pr} > 1$. Assuming again that the bulk dominates the viscous dissipation:

$$\mathrm{Ra\,Nu} = \mathrm{Pr}^{2/3}\mathrm{ReNu}^3 = \mathrm{Re}^3\mathrm{Pr}^2. \tag{49}$$

Using equation (40):

$$\mathrm{Nu}^3 = \mathrm{Re}^2\mathrm{Pr}^{4/3} = \mathrm{Nu}^{4-2\alpha} \tag{50}$$

and $\alpha = 0.5$. Moreover, in both cases, this model agrees with our assumption, equation (19).

The following argument could give an idea on the spectrum of other possible α values.

Let us call α_1 the first possible value for α. Above the transition from $\alpha = 0$ to $\alpha = \alpha_1$, as Nu increases, and δ goes down, the development length h could act as an effective large scale, the flow being confined between two neighboring plumes. Then, a new step of the instability of the thermal boundary layer could develop, yielding a new development length h'. The relation between h and h' would then write:

$$\frac{h}{h'} = \left(\frac{h}{\delta}\right)^{\alpha_1} \tag{51}$$

or:

$$\frac{h}{H}\frac{H}{h'} = \mathrm{Nu}^{-\alpha_{n-1}}\frac{H}{h'} = \left(\frac{h}{H}\frac{H}{\delta}\right)^{\alpha_1} = (\mathrm{Nu}^{1-\alpha_{n-1}})^{\alpha_1} \tag{52}$$

It gives the following recursion formula:

$$(1-\alpha_n) = (1-\alpha_{n-1})(1-\alpha_1). \tag{53}$$

Table 1. Important relations for the development length h.

	Small Pr	**Large Pr**
Postulated	$H/h = \mathrm{Nu}^{\alpha}$	$H/h = \mathrm{Nu}^{\alpha}$
Derived	$H/h = \mathrm{Nu}^2/\mathrm{Re\,Pr}$	$H/h = \mathrm{Nu}^2/\mathrm{Re\,Pr}^{2/3}$
Observed		$H/h = L_p H/S$ [28]
Observed α values		$\alpha = 0.3$; $\alpha = 0.77$ [10] $\alpha = 0.48$ [14] $\alpha = 0.77$ [28]
Derived α values	$\alpha = 0.5$ [15]	$\alpha = 0.5$ [13] $\alpha = 0.5$; $\alpha = 0.75$ (this work)

Identifying the Kadanoff α value, 0.5, with α_1, the following value would be 0.75, very close to the observed ones, 0.77 for the Chavanne et al. [10] or Musilova et al. [21] data, or 0.76 for the Puthenveettil et al. [28] ones.

Note that for the lowest α value observed, 0.30, the viscous dissipation is dominated by the boundary layer, in contradiction with the hypothesis of the Kadanoff et al. model [13,15].

6. The viscous dissipation

In this section we shall determine the viscous dissipation in the velocity boundary layer, and in the bulk. Using then equation (12), we shall identify $(\mathrm{Nu}-1)$ with Nu, as the difference is smaller than the error bar in the experimental or numerical studies of the concerned regimes. A constant reference for the mean viscous dissipation per unit mass will be (see equation (15)):

$$\frac{U^3}{H} = \frac{\kappa^3}{H^4}\mathrm{Re}^3\mathrm{Pr}^3. \tag{54}$$

6.1. *The boundary layer contribution*

We have here to distinguish between a Blasius type boundary layer and a logarithmic one.

6.1.1. *The Blasius case*

Then, λ, the width of the velocity boundary layer, is the momentum diffusion length during a time h/U:

$$\lambda = \sqrt{\frac{\nu h}{U}} = H\mathrm{Nu}^{-\alpha/2}\mathrm{Re}^{-1/2}, \tag{55}$$

$$\gamma = \frac{U}{\lambda} = \frac{\nu}{H^2}\mathrm{Nu}^{\alpha/2}\mathrm{Re}^{3/2}. \tag{56}$$

The boundary layer contribution to the viscous dissipation per unit mass will thus be:

$$\varepsilon_{\mathrm{bl}} = \frac{\lambda}{H}\nu\gamma^2 = \frac{\nu^3}{H^4}\mathrm{Nu}^{\alpha/2}\mathrm{Re}^{5/2}. \tag{57}$$

When this contribution dominates, comparing with equation (12) gives:

$$\mathrm{Ra\,Nu} = \mathrm{Nu}^{\alpha/2}\mathrm{Re}^{5/2}\mathrm{Pr}^2. \tag{58}$$

Another expression can be derived in this Blasius case. Namely:

$$\varepsilon_{\rm bl} = \frac{\lambda}{H}\nu\frac{U^2}{\lambda^2} = \frac{\nu^3}{H^4}{\rm Re}^2\frac{H}{\lambda}. \tag{59}$$

Assuming that both the thermal and the viscous dissipations are dominated by the boundary layer, and using equations (12), (34) and (31), it gives, for small Prandtl numbers:

$${\rm Ra\,Nu} = {\rm Nu\,Re}^2{\rm Pr}^{3/2}, \tag{60}$$

and for large Prandtl numbers:

$${\rm Ra\,Nu} = {\rm Nu\,Re}^2{\rm Pr}^{5/3}. \tag{61}$$

These expressions have the advantage to be independent of α.

6.1.2. *The logarithmic case*

Again, we have to take into account the development length h. In the viscous sublayer, the horizontal velocity component is $u_x = \gamma z$, with:

$$\gamma = v_*^2/\nu, \tag{62}$$

the transverse momentum flux being ρv_*^2 by definition of v_*. As above, the vertical velocity component u_z can be derived from the incompressibility relation (2):

$$\partial_z u_z = -\partial_x u_x = \frac{\gamma z}{h}, \quad u_z = \frac{\gamma z^2}{h} \tag{63}$$

(we omit the factor 2).

In the logarithmic range (see, for instance, [30]),

$$\partial_z u_x = \frac{v_*}{z}, \quad u_x = v_*\ln\left(\frac{v_* z}{\nu}\right), \quad U = v_*\ln({\rm Re}) \tag{64}$$

(we omit the von Karman constant).

The velocity sublayer limit $z = \lambda$ corresponds to the transition viscous-convective for the momentum flux. In the convective region, $\langle u_x u_z\rangle = v_*^2 \simeq \sqrt{\langle u_x^2\rangle\langle u_z^2\rangle}$, assuming again a constant correlation coefficient. In the viscous region, $\sqrt{\langle u_x^2\rangle} \simeq \gamma z$, $\sqrt{\langle u_z^2\rangle} \simeq \gamma z^2/h$. Thus, at the transition:

$$v_*^2 = \frac{\gamma^2\lambda^3}{h}, \quad \frac{v_*^3\lambda^3}{\nu^3} = y_+^3(\lambda) = \frac{v_* h}{\nu} = \frac{{\rm ReNu}^{-\alpha}}{\ln({\rm Re})} = D, \tag{65}$$

$y_+ = v_* z/\nu$ being the traditional notation for the reduced distance to the plate [30].

The above result strongly suggests that $D = 1$. Indeed, to our knowledge, no experimental results show a dependence of the reduced distance y_+ at the top of the viscous sublayer with the Reynolds number. This is the option we shall take.

Then the contribution of the viscous sublayer to the viscous dissipation is:

$$\frac{\lambda}{H}\nu\gamma^2 = \frac{v_*^3}{H} = \frac{U^3}{H(\ln{\rm Re})^3}, \tag{66}$$

while that of the logarithmic part is:

$$\frac{1}{H}\int_\lambda^H \langle u_x u_z\rangle\partial_z u_x {\rm d}z = \frac{v_*^3}{H}\ln{\rm Re} = \frac{U^3}{H(\ln{\rm Re})^2}. \tag{67}$$

The latter being larger, we shall take it as the contribution of the logarithmic boundary layer. If it dominates the total viscous dissipation, we have:

$${\rm Ra\,Nu} = \frac{{\rm Re}^3{\rm Pr}^2}{(\ln{\rm Re})^2}. \tag{68}$$

Remark 1 (On the relation between λ and δ). Note that the above results have consequences both in the relation between the velocity boundary layer λ and the thermal one δ, and in the relation between the typical bulk temperature fluctuation Θ and Nu and Re.

As remarked above, our relations (34) and (31) are valid only if $h \gg \delta$. In the logarithmic case, the velocity vertical component fluctuation does not grow when $z > \lambda$, and remains of order v_*. For low Prandtl numbers in the logarithmic case, it implies:

$$\delta = \frac{\lambda}{\mathrm{Pr}}. \tag{69}$$

For $\mathrm{Pr} > 1$ in the same case, let us remark that equation (23) implies, when $h \simeq \delta$:

$$\delta^2 = \frac{\kappa}{\gamma}. \tag{70}$$

Then, using equation (62):

$$\delta^2 = \frac{\kappa\nu}{v_*^2} = \frac{\lambda^2}{\mathrm{Pr}}. \tag{71}$$

Kraichnan [25] obtained the same relation, assuming that the vertical velocity fluctuation is linear in z for $z < \lambda$, at least for not too small z.

However, as Kraichnan himself remarked, such a regime cannot hold for large Prandtl numbers. The reason is that, as pointed above (see equation (63)), the vertical velocity must be quadratic in z close to the plates. Using equation (65) :

$$\frac{\delta}{h} = \frac{\delta}{\lambda}\frac{\lambda}{h} = D^{-2/3}\mathrm{Pr}^{-1/2}. \tag{72}$$

Thus the condition $h \simeq \delta$ cannot hold for large Pr, where the relation between λ and δ is, as in the Blasius case (see equation (31)):

$$\lambda = \delta \mathrm{Pr}^{1/3}. \tag{73}$$

We shall call "Kraichnan range" the limited range of Prandtl numbers (if it even exists), close to 1, where equation (71) holds.

Remark 2 (On the relation between Θ and Nu, Re). As for the relation between the typical bulk temperature fluctuation Θ and Nu and Re, as the velocity vertical component fluctuation does not grow when $z > \lambda$, and remains of order v_*, we should have:

$$\langle u_z \theta \rangle = v_* \Theta. \tag{74}$$

Then:

$$\mathrm{Nu} = \frac{\langle u_z\theta\rangle}{\kappa\Delta} = \frac{v_* H}{\nu}\frac{\nu}{\kappa}\frac{\Theta}{\Delta}, \tag{75}$$

and:

$$\frac{\Theta}{\Delta} = \frac{\mathrm{Nu}(\ln \mathrm{Re})}{\mathrm{Re}\,\mathrm{Pr}}, \tag{76}$$

which substitutes to equation (17) with constant χ for logarithmic boundary layers.

6.2. *The bulk contribution*

In the bulk, we shall follow the estimation by GL [7] and determine the bulk contribution as U^3/H, both in the Blasius and in the logarithmic cases. It comes from the interaction between rising and falling plumes. If this contribution dominates, we have (see equation (15)):

$$\mathrm{Ra}\,\mathrm{Nu} = \mathrm{Re}^3\mathrm{Pr}^2. \tag{77}$$

We can now compare with the experimental results. Indeed, the quantity:

$$\mathrm{DVB} = \frac{\mathrm{Re}^3\mathrm{Pr}^2}{\mathrm{Ra}\,\mathrm{Nu}} \tag{78}$$

represents, within a constant factor, the part of the viscous dissipation which is due to the bulk, while the quantities:

$$\mathrm{DVL}_l = \frac{\mathrm{Re}^2\mathrm{Pr}^{3/2}}{\mathrm{Ra}} \tag{79}$$

(see equation (60)) for small Prandtl numbers, or:

$$\mathrm{DVL}_u = \frac{\mathrm{Re}^2\mathrm{Pr}^{5/3}}{\mathrm{Ra}} \tag{80}$$

(see equation (61)) for large Prandtl numbers, represent, again within a constant factor, the part of the viscous dissipation which is due to the boundary layer. We let aside, for the moment, the logarithmic boundary layer case.

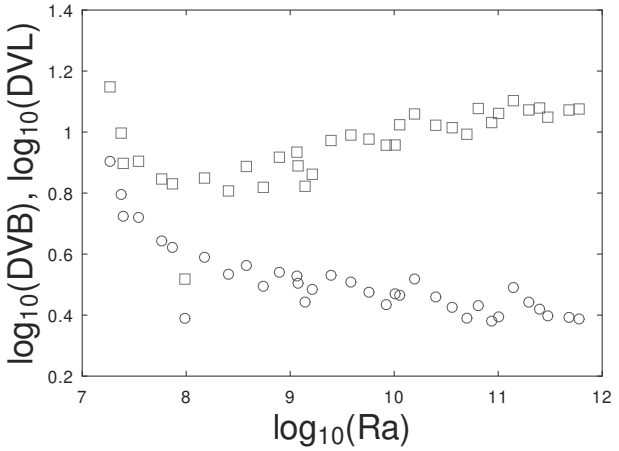

Figure 7. The respective parts of the viscous dissipation in the bulk (DVB, squares), and in the boundary layer (DVL_u, circles), for the X. Z. Wu results, using equations (78) and (80). A vertical shift has been applied for clarity.

On Figure 7, we show these two quantities, versus the Rayleigh number, in logarithmic scales, for the X. Z. Wu results. None of these quantities shows a plateau. The part of the bulk dissipation increases with Nu, while the part of the boundary layer decreases. This is an excellent illustration of the GL point of view, a slow cross-over between the two regimes.

On Figure 8, we show the same quantities, versus the Rayleigh number, in logarithmic scales, for the Chavanne et al. results. While it is clear that the first regime, with $\alpha = 0.30$, is dominated by the boundary layer, the second regime seems to give a plateau in both cases. We are unable to decide between the bulk or the boundary layer dominating the viscous dissipation.

7. The thermal boundary layer δ

Indeed, the determination of λ in the previous section gives the thermal boundary layer δ as a by-product. Let us first recall the results for λ. In the Blasius case:

$$\lambda = H\mathrm{Nu}^{-\alpha/2}\mathrm{Re}^{-1/2}, \tag{81}$$

while, in the logarithmic boundary layer case:

$$\lambda = \frac{\nu}{v_*} = H\frac{\ln(\mathrm{Re})}{\mathrm{Re}}. \tag{82}$$

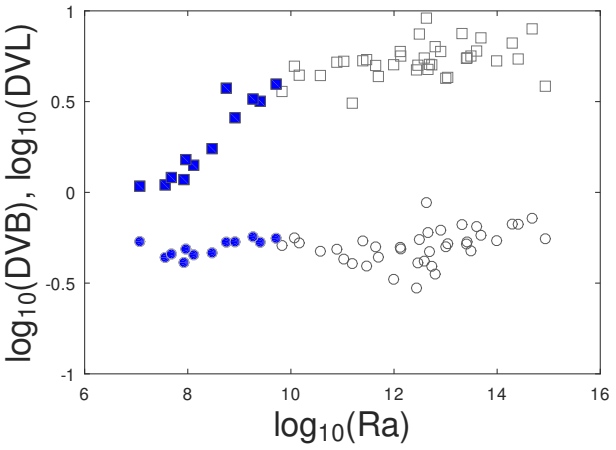

Figure 8. The respective parts of the viscous dissipation in the bulk (DVB, squares), and in the boundary layer (DVL_u, circles), for the Chavanne et al. results, using equations (78) and (80). A vertical shift has been applied for clarity. Full symbols correspond to the first regime ($\alpha \simeq 0.3$).

In the Blasius case, following our previous analysis, Section 6.1, for small Prandtl numbers:

$$\delta = \frac{\lambda}{\mathrm{Pr}^{1/2}}, \tag{83}$$

while, for large Prandtl numbers:

$$\delta = \frac{\lambda}{\mathrm{Pr}^{1/3}}. \tag{84}$$

Reciprocally, in the logarithmic boundary layer case, for small Prandtl numbers:

$$\delta = \frac{\lambda}{\mathrm{Pr}}, \tag{85}$$

and, for large Prandtl numbers:

$$\delta = \frac{\lambda}{\mathrm{Pr}^{1/3}}, \tag{86}$$

except for a small range of Prandtl numbers, close to 1 (the Kraichnan range), where (see equation (71)):

$$\delta = \frac{\lambda}{\mathrm{Pr}^{1/2}}. \tag{87}$$

Table 2. Relations between λ and δ.

	Blasius boundary layer	**Logarithmic boundary layer**
Low Pr	$\lambda = \delta \mathrm{Pr}^{1/2} = H\mathrm{Nu}^{-\alpha/2}\mathrm{Re}^{-1/2}$	$\lambda = \delta \mathrm{Pr} = H\mathrm{Re}^{-1}\ln(\mathrm{Re})$
Kraichnan range	$\lambda = \delta \mathrm{Pr}^{1/3} = H\mathrm{Nu}^{-\alpha/2}\mathrm{Re}^{-1/2}$	$\lambda = \delta \mathrm{Pr}^{1/2} = H\mathrm{Re}^{-1}\ln(\mathrm{Re})$
Large Pr	$\lambda = \delta \mathrm{Pr}^{1/3} = H\mathrm{Nu}^{-\alpha/2}\mathrm{Re}^{-1/2}$	$\lambda = \delta \mathrm{Pr}^{1/3} = H\mathrm{Re}^{-1}\ln(\mathrm{Re})$

Table 3. Important relations for viscous dissipation. BL = boundary layer.

Flow's dominant part		
Blasius BL	Logarithmic BL	Bulk
$\mathrm{Ra}\,\mathrm{Nu} = \mathrm{Nu}^{\alpha/2}\mathrm{Re}^{5/2}\mathrm{Pr}^2$	$\mathrm{Ra}\,\mathrm{Nu} = \mathrm{Re}^3\mathrm{Pr}^2/\left(\ln(\mathrm{Re})\right)^2$	$\mathrm{Ra}\,\mathrm{Nu} = \mathrm{Re}^3\mathrm{Pr}^2$

8. The thermal dissipation

8.1. *The boundary layer contribution*

The boundary layer contribution is simply given by:

$$\kappa\left(\frac{\Delta}{\delta}\right)^2\frac{\delta}{H} = \kappa\left(\frac{\Delta}{H}\right)^2\frac{H}{\delta}. \tag{88}$$

When the thermal dissipation is dominated by the boundary layer, equation (13) yields an identity. We could refer to our determination of the boundary layer δ, for instance through equations (39) or (40), but we must remember that we used it to determine α, and thus it is identically verified.

The only check we have is thus to look at the bulk contribution. If the bulk contribution is constant, we shall conclude that it dominates the thermal dissipation. If it is not constant, we shall conclude that a significant boundary layer contribution exists. We have no possible cross-check.

8.1.1. *The temperature profile*

Moreover, considering that the boundary layer contribution is only part of the total thermal dissipation implies that the temperature difference across the boundary layer, $\Delta^*/2$, differs from $\Delta/2$. Let us call Nu^* the boundary layer contribution to the thermal dissipation normalized by $\kappa(\Delta/H)^2$:

$$\frac{\kappa}{4}\left(\frac{\Delta^*}{\delta}\right)^2\frac{2\delta}{H} = \frac{\kappa\Delta^2}{H^2}\left(\frac{\Delta^*}{\Delta}\right)^2\frac{H}{2\delta} = \frac{\kappa\Delta^2}{H^2}\mathrm{Nu}^*. \tag{89}$$

As:

$$\frac{\Delta^*}{2} = \delta\frac{\dot{Q}}{\kappa C_p} = \frac{\delta}{H}\Delta\mathrm{Nu}, \tag{90}$$

we have:

$$\frac{\Delta^*}{\Delta} = \frac{2\delta}{H}\mathrm{Nu} \tag{91}$$

and:

$$\mathrm{Nu}^* = \frac{\Delta^*}{\Delta}\mathrm{Nu}, \tag{92}$$

which means that the boundary layer contribution is in the same proportion as the temperature differences. It is then interesting to look at the temperature profile in the convective part of the convection cell.

The situation is indeed very similar to that yielding to the turbulent logarithmic velocity profile. $\Theta = \Delta\mathrm{Nu}/\mathrm{Re}\,\mathrm{Pr}$ acts as a typical temperature difference, while, at a distance z from the plate, there is no other characteristic length than z. From dimensional analysis, the mean vertical temperature gradient must write:

$$\left\langle\frac{\partial T}{\partial z}\right\rangle = \varpi\frac{\Theta}{z}, \tag{93}$$

where ϖ is a universal constant, similar to the von Karman constant. However, our arguments are independent of the velocity boundary layer being turbulent or of the Blasius type.

Then $\langle T\rangle = \varpi\Theta\ln(z) + \text{cst}$ and $\Delta - \Delta^* \simeq \varpi\Theta\ln(\text{Nu})$. Note that such a logarithmic temperature profile has been effectively observed in some studies [31].

Thus, the evolution is slow, and Δ cannot be much larger than Δ^* before extremely large values of Nu be reached. In practical situations, the boundary layer contribution is always a noticeable part of the total thermal dissipation. Rather than a dissipation "dominated" by the bulk, we should speak of a dissipation "driven" by the bulk, as the boundary layer adapts to follow the bulk contribution.

8.2. *The bulk contribution*

Following the approach of [12], we shall determine the bulk contribution to the thermal dissipation through:

$$\kappa\langle\partial_i T\partial_i T\rangle \simeq \kappa\left(\frac{\vartheta}{\sigma}\right)^2, \tag{94}$$

where ϑ is the temperature fluctuation at the thermal dissipative scale σ. As in [12], we have to distinguish between hard and soft turbulence, and large or small Prandtl numbers.

8.2.1. *Small Prandtl numbers. Hard turbulence*

When the inertial turbulent cascade is sufficiently developed, the thermal dissipative scale σ, while larger than the viscous one η ($\text{Pr} < 1$), is in the inertial range: $H > \sigma > \eta$. At the scale σ, the thermal diffusion time is equal to the stretching time. Put in other words, the Peclet number is 1:

$$\frac{\kappa}{\sigma^2} = \frac{v_\sigma}{\sigma}. \tag{95}$$

Using the Kolmogorov 41 theory [32]:

$$\frac{H}{\sigma} = \frac{H}{\kappa}U\left(\frac{H}{\sigma}\right)^{1/3}, \quad \frac{H}{\sigma} = \left(\frac{UH}{\kappa}\right)^{3/4} = (\text{Re}\,\text{Pr})^{3/4}. \tag{96}$$

As for the temperature fluctuations:

$$\vartheta = \Theta\left(\frac{\sigma}{H}\right)^{1/3} = \Theta(\text{Re}\,\text{Pr})^{-1/4}. \tag{97}$$

Using equations (94) and (17), the bulk contribution to the thermal dissipation is then:

$$\kappa\left(\frac{\Delta}{H}\right)^2\left(\frac{\Theta}{\Delta}\right)^2(\text{Re}\,\text{Pr})^{-1/2}(\text{Re}\,\text{Pr})^{3/2} = \kappa\left(\frac{\Delta}{H}\right)^2\frac{\text{Nu}^2}{\text{Re}\,\text{Pr}}. \tag{98}$$

Note that we could have obtained this result, identifying the thermal dissipation ϵ_T with $U\Theta^2/H$, as GL did [7]. $U\Theta^2/H$ is the large scale expression of ϵ_T, and the cascade ensures the conservation of ϵ_T:

$$\frac{U\Theta^2}{H} = \kappa\left(\frac{\Delta}{H}\right)^2\frac{UH}{\nu}\frac{\nu}{\kappa}\frac{\Theta^2}{\Delta^2}. \tag{99}$$

If this contribution dominates, using equation (13) gives:

$$\text{Nu} = \text{Re}\,\text{Pr}, \quad \frac{\Theta}{\Delta} = \text{cst}. \tag{100}$$

If the bulk viscous dissipation also dominates, using equation (77) gives:

$$\text{Re} = \text{Ra}^{1/2}\text{Pr}^{-1/2}, \quad \text{Nu} = \text{Ra}^{1/2}\text{Pr}^{1/2}. \tag{101}$$

8.2.2. *Very small Prandtl numbers. Hard turbulence*

We consider this case, inspired by the recent paper of Shishkina and Lohse [33]. These authors correctly remark that, for $\mathrm{Pr} < \mathrm{Ra}^{-1}$, equation (101) would imply a Nusselt number going to zero. Indeed, Nu doesn't go to zero. When it goes close to one, we must go back to equation (12). If the bulk viscous dissipation dominates, equation (77) becomes:

$$\mathrm{Ra}\,(\mathrm{Nu}-1) = \mathrm{Re}^3\mathrm{Pr}^2. \tag{102}$$

As:

$$\dot{Q} = C_p\left(\kappa\frac{\Delta}{H} + \langle u_z\theta\rangle\right), \tag{103}$$

we can now estimate Θ through:

$$\frac{\Theta}{\Delta} = \frac{\mathrm{Nu}-1}{\mathrm{Re}\,\mathrm{Pr}}. \tag{104}$$

Equations (13), (99), (104) give:

$$\frac{U\Theta^2}{H} = \kappa\left(\frac{\Delta}{H}\right)^2\mathrm{Re}\,\mathrm{Pr}\left(\frac{\mathrm{Nu}-1}{\mathrm{Re}\,\mathrm{Pr}}\right)^2 = \kappa\left(\frac{\Delta}{H}\right)^2\mathrm{Nu}. \tag{105}$$

Using equations (102), (105) and $\mathrm{Nu} \simeq 1$, $(\mathrm{Nu}-1) = (\mathrm{Re}\,\mathrm{Pr})^{1/2}$, and:

$$\mathrm{Re} = \mathrm{Ra}^{2/5}\mathrm{Pr}^{-3/5}, \quad \mathrm{Nu}-1 = \mathrm{Ra}^{1/5}\mathrm{Pr}^{1/5}. \tag{106}$$

8.2.3. *Small Prandtl numbers. Intermediate turbulence*

For smaller Reynolds numbers, the thermal dissipative scale σ is out of the inertial range. Then, we must identify it with H. The bulk contribution to the thermal dissipation is then:

$$\kappa\left(\frac{\Theta}{H}\right)^2 = \kappa\left(\frac{\Delta}{H}\right)^2\left(\frac{\Theta}{\Delta}\right)^2 = \kappa\left(\frac{\Delta}{H}\right)^2\left(\frac{\mathrm{Nu}}{\mathrm{Re}\,\mathrm{Pr}}\right)^2. \tag{107}$$

If this contribution dominates, using equation (13) gives:

$$\mathrm{Nu} = (\mathrm{Re}\,\mathrm{Pr})^2, \quad \frac{\Theta}{\Delta} = \mathrm{Re}\,\mathrm{Pr}. \tag{108}$$

If the bulk viscous dissipation also dominates, using equation (77) gives:

$$\mathrm{Nu} = (\mathrm{Re}\,\mathrm{Pr})^2 = (\mathrm{Ra}\,\mathrm{Pr})^2, \quad \frac{\Theta}{\Delta} = \mathrm{Re}\,\mathrm{Pr}. \tag{109}$$

8.2.4. *Arbitrary Prandtl numbers. Soft turbulence*

In this case, while turbulent, the bulk has no inertial energy cascade. As in [12], we then determine the temperature dissipation scale σ, writing that the inverse temperature diffusion time is equal to the velocity gradient, itself determined through the dissipation:

$$\frac{\kappa}{\sigma^2} = \sqrt{\frac{\varepsilon}{\nu}}. \tag{110}$$

The bulk contribution to the thermal dissipation is then, both for small and large Prandtl numbers:

$$\begin{aligned}\kappa\frac{\langle\theta^2\rangle}{\sigma^2} &= \langle\theta^2\rangle\sqrt{\frac{\varepsilon}{\nu}}\\ &= \Delta^2\frac{\mathrm{Nu}^2}{\mathrm{Re}^2\mathrm{Pr}^2}\sqrt{\frac{\kappa^3\mathrm{Re}^3\mathrm{Pr}^3}{H^4\nu}}\\ &= \kappa\left(\frac{\Delta}{H}\right)^2\frac{\mathrm{Nu}^2}{\mathrm{Re}^{1/2}\mathrm{Pr}}.\end{aligned} \tag{111}$$

If this contribution dominates, we have, for arbitrary Prandtl numbers:

$$\mathrm{Nu} = \mathrm{Re}^{1/2}\mathrm{Pr}, \quad \frac{\Theta}{\Delta} = \mathrm{Pr}\,\mathrm{Nu}^{-1}. \tag{112}$$

If the bulk viscous dissipation also dominates (GL case (IV)), equations (112) and (77) give:

$$\mathrm{Re} = \mathrm{Ra}^{2/5}\mathrm{Pr}^{-2/5}, \quad \mathrm{Nu} = \mathrm{Ra}^{1/5}\mathrm{Pr}^{4/5}. \tag{113}$$

8.2.5. *Large Prandtl numbers. Hard turbulence*

In this case, an inertial range exists, but the thermal dissipative scale σ is smaller than the viscous dissipation scale η. These scales are related through:

$$\frac{\kappa}{\sigma^2} = \frac{v_\sigma}{\sigma} = \frac{v_\eta}{\eta} = \frac{\nu}{\eta^2}. \tag{114}$$

This regime is known as the Batchelor regime [12]. The temperature fluctuation at the thermal dissipative scale σ is the same as at the viscous dissipative scale η:

$$\vartheta = \Theta\left(\frac{\eta}{H}\right)^{1/3} = \Theta\mathrm{Re}^{-1/4}. \tag{115}$$

The bulk contribution to the thermal dissipation is then:

$$\begin{aligned}\kappa\left(\frac{\vartheta}{\sigma}\right)^2 &= \kappa\left(\frac{\Delta}{H}\right)^2\left(\frac{\Theta}{\Delta}\right)^2\left(\frac{\vartheta}{\Theta}\right)^2\left(\frac{H}{\eta}\right)^2\left(\frac{\eta}{\sigma}\right)^2 \\ &= \kappa\left(\frac{\Delta}{H}\right)^2\left(\frac{\Theta}{\Delta}\right)^2 \mathrm{Re}\,\mathrm{Pr} \\ &= \kappa\left(\frac{\Delta}{H}\right)^2 \frac{\mathrm{Nu}^2}{\mathrm{Re}\,\mathrm{Pr}}.\end{aligned} \tag{116}$$

This result is identical to what we obtained in the low Prandtl numbers case, equation (99), for the same reasons. We shall show below that, as a consequence of the recently derived bounds by Choffrut et al. [34], such a bulk dissipation cannot exceed the boundary layer thermal dissipation for arbitrarily large Rayleigh numbers.

Choffrut et al. derived two bounds for Nu in the large Pr case:

$$\mathrm{Nu} < \mathrm{Ra}^{1/2}\mathrm{Pr}^{-1/2}, \tag{117}$$

for $\mathrm{Pr} < \mathrm{Ra}^{1/3}$, and:

$$\mathrm{Nu} < \mathrm{Ra}^{1/3}, \tag{118}$$

for $\mathrm{Pr} > \mathrm{Ra}^{1/3}$.

Assume that the bulk thermal dissipation, equation (116), be larger than the boundary layer one, equation (88). It would mean, for large Reynolds numbers:

$$\begin{aligned}\frac{\mathrm{Nu}^2}{\mathrm{Re}\,\mathrm{Pr}} > \frac{H}{\delta} = \mathrm{Re}\,\mathrm{Pr}^{1/3}, \\ \mathrm{Nu}^2 > \mathrm{Re}^2\mathrm{Pr}^{4/3}.\end{aligned} \tag{119}$$

Using equation (77):

$$\begin{aligned}\mathrm{Ra}\,\mathrm{Nu} = \mathrm{Re}^3\mathrm{Pr}^2 > \mathrm{Ra}\,\mathrm{Re}\,\mathrm{Pr}^{2/3}, \\ \mathrm{Re}^2\mathrm{Pr}^{4/3} > \mathrm{Ra}.\end{aligned} \tag{120}$$

Using equation (117) ($\mathrm{Pr} < \mathrm{Ra}^{1/3}$):

$$\mathrm{Re}^2\mathrm{Pr}^{1/3} > \mathrm{Ra}\,\mathrm{Pr}^{-1} > \mathrm{Nu}^2 > \mathrm{Re}^2\mathrm{Pr}^{4/3}, \tag{121}$$

which is impossible at large Pr.

Using equation (118) ($\mathrm{Pr} > \mathrm{Ra}^{1/3}$) and equation (119):

$$\begin{aligned} \mathrm{Ra} &> \mathrm{Nu}^3 > \mathrm{Re}^3\mathrm{Pr}^2 = \mathrm{Ra}\,\mathrm{Nu}, \\ \mathrm{Nu}^2 &> \mathrm{Ra}, \end{aligned} \tag{122}$$

which violates equation (118).

Thus, in each case, the thermal dissipation is dominated by the boundary layer.

Table 4. Important relations for thermal dissipation. BL = boundary layer.

Flow's dominant part	Low Prandtl numbers	Kraichnan range	Large Prandtl numbers
Blasius BL	$\mathrm{Nu} = \mathrm{Nu}^{\alpha/2}\mathrm{Re}^{1/2}\mathrm{Pr}^{1/2}$	$\mathrm{Nu} = \mathrm{Nu}^{\alpha/2}\mathrm{Re}^{1/2}\mathrm{Pr}^{1/2}$	$\mathrm{Nu} = \mathrm{Nu}^{\alpha/2}\mathrm{Re}^{1/2}\mathrm{Pr}^{1/3}$
Logarithmic BL	$\mathrm{Nu} = \mathrm{Re}\,\mathrm{Pr}/\ln(\mathrm{Re})$	$\mathrm{Nu} = \mathrm{Re}\,\mathrm{Pr}^{1/2}/\ln(\mathrm{Re})$	$\mathrm{Nu} = \mathrm{Re}\,\mathrm{Pr}^{1/3}/\ln(\mathrm{Re})$
Bulk Soft turb	$\mathrm{Nu} = \mathrm{Nu}^2\mathrm{Re}^{-1/2}\mathrm{Pr}^{-1/2}$	$\mathrm{Nu} = \mathrm{Nu}^2\mathrm{Re}^{-1/2}\mathrm{Pr}^{-1/2}$	$\mathrm{Nu} = \mathrm{Nu}^2\mathrm{Re}^{-1/2}\mathrm{Pr}^{-1/2}$
Bulk Intermediate turb	$\mathrm{Nu} = \mathrm{Nu}^2\mathrm{Re}^{-2}\mathrm{Pr}^{-2}$	Not dominant	Not dominant
Bulk Hard turb	$\mathrm{Nu} = \mathrm{Nu}^2\mathrm{Re}^{-1}\mathrm{Pr}^{-1}$	Not dominant	Not dominant

9. Discussion

We can now obtain the scalings of Nu, Re, and Θ/Δ in all "pure" regimes. Such an enumeration would however be tedious, as we have to distinguish not only all the GL regimes, but also if the Prandtl number is large or small, if the boundary layer is Blasius or logarithmic, and if the turbulence in the bulk is hard or soft. We prefer to detail some remarkable cases, to show how these scalings can be obtained.

9.1. *The Kadanoff solution*

This case corresponds to a bulk dominated viscous dissipation, and a thermal dissipation dominated by a Blasius boundary layer. The value of α is $\alpha = 1/2$.

Equation (77) gives:

$$\mathrm{Ra}\,\mathrm{Nu} = \mathrm{Re}^3\mathrm{Pr}^2. \tag{123}$$

At large Prandtl number, equations (81) and (84) give:

$$\begin{aligned} \mathrm{Nu} &= \frac{H}{\delta} = \mathrm{Nu}^{\alpha/2}\mathrm{Re}^{1/2}\mathrm{Pr}^{1/3}, \\ \mathrm{Nu} &= \mathrm{Re}^{1/(2-\alpha)}\mathrm{Pr}^{2/3(2-\alpha)}. \end{aligned} \tag{124}$$

Then:

$$\mathrm{Re} = \mathrm{Ra}^{(2-\alpha)/(5-3\alpha)}\mathrm{Pr}^{-2/3}, \tag{125}$$

$$\mathrm{Nu} = \mathrm{Ra}^{1/(5-3\alpha)}, \tag{126}$$

$$\frac{\Theta}{\Delta} = \mathrm{Ra}^{(\alpha-1)/(5-3\alpha)}\mathrm{Pr}^{-1/3}, \tag{127}$$

which, for $\alpha = 1/2$, gives:

$$\mathrm{Re} = \mathrm{Ra}^{3/7}\mathrm{Pr}^{-2/3}, \quad \mathrm{Nu} = \mathrm{Ra}^{2/7}, \quad \frac{\Theta}{\Delta} = \mathrm{Ra}^{-1/7}\mathrm{Pr}^{-1/3}. \tag{128}$$

The Cioni et al. [15] extension of this regime to small Prandtl numbers corresponds to using equation (83) instead of (84):

$$\begin{aligned} \mathrm{Nu} &= \frac{H}{\delta} = \mathrm{Nu}^{\alpha/2}\mathrm{Re}^{1/2}\mathrm{Pr}^{1/2}, \\ \mathrm{Nu} &= \mathrm{Re}^{1/(2-\alpha)}\mathrm{Pr}^{1/(2-\alpha)}. \end{aligned} \tag{129}$$

Then:

$$\mathrm{Re} = \mathrm{Ra}^{(2-\alpha)/(5-3\alpha)}\mathrm{Pr}^{-(3-2\alpha)/(5-3\alpha)}, \tag{130}$$

$$\mathrm{Nu} = \mathrm{Ra}^{1/(5-3\alpha)}\mathrm{Pr}^{1/(5-3\alpha)}, \tag{131}$$

$$\frac{\Theta}{\Delta} = \mathrm{Ra}^{(\alpha-1)/(5-3\alpha)}\mathrm{Pr}^{(5\alpha-1)/(5-3\alpha)}, \tag{132}$$

which, for $\alpha = 1/2$, gives:

$$\mathrm{Re} = \mathrm{Ra}^{3/7}\mathrm{Pr}^{-4/7}, \quad \mathrm{Nu} = \mathrm{Ra}^{2/7}\mathrm{Pr}^{2/7}, \quad \frac{\Theta}{\Delta} = \mathrm{Ra}^{-1/7}\mathrm{Pr}^{3/7}. \tag{133}$$

While the final regime of Wu results gives $\alpha = 1/2$, we cannot identify this regime with the Kadanoff one. The reason is that the bulk relative part of the viscous dissipation is not constant, as can be seen on Figure 7, which shows that the boundary layer part is significant. For a boundary layer part dominant, instead of equation (77), we should have (see equation (58)):

$$\mathrm{Ra}\,\mathrm{Nu} = \mathrm{Nu}^{\alpha/2}\mathrm{Re}^{5/2}\mathrm{Pr}^{2}. \tag{134}$$

Together with equations (81) and (84), it gives:

$$\mathrm{Re} = \mathrm{Ra}^{1/2}\mathrm{Pr}^{-5/6}, \tag{135}$$

and, using $\alpha = 1/2$:

$$\mathrm{Nu} = \mathrm{Ra}^{1/3}\mathrm{Pr}^{-1/9}. \tag{136}$$

As GL proposed [7], this final regime of Wu results presents a crossover between the above regime and the Kadanoff one.

In their paper, Castaing et al. compared Θ/Δ and Nusselt. The two above equations give:

$$\frac{\Theta}{\Delta} = \frac{\mathrm{Nu}}{\mathrm{Re}\,\mathrm{Pr}} = \mathrm{Nu}^{-1/2}\mathrm{Pr}^{-7/18}, \tag{137}$$

while the Kadanoff solution gives:

$$\frac{\Theta}{\Delta} = \frac{\mathrm{Nu}}{\mathrm{Re}\,\mathrm{Pr}} = \mathrm{Nu}^{-1/2}\mathrm{Pr}^{-1/3}. \tag{138}$$

The difference is too small to conclude.

9.2. *The Kraichnan solution*

In a celebrated paper [25], R. Kraichnan proposed a large Rayleigh numbers regime for moderately large Prandtl numbers, which has long been understood as the "ultimate" regime. Each thermal boundary layer is supposed to have half the total temperature difference Δ across it, in agreement with the conclusions of Section 8.2.5, and the Choffrut et al. [34] bounds.

On the one hand, we again have, using equation (77):

$$\mathrm{Ra}\,\mathrm{Nu} = \mathrm{Re}^{3}\mathrm{Pr}^{2}. \tag{139}$$

On the other hand, using equations (71) and (82) we obtain:

$$\mathrm{Nu} = \frac{H}{\delta} = \frac{\mathrm{Re}\,\mathrm{Pr}^{1/2}}{\ln(\mathrm{Re})}. \tag{140}$$

It gives:

$$\mathrm{Re} = \frac{\mathrm{Ra}^{1/2}\mathrm{Pr}^{-3/4}}{\left(\ln(\mathrm{Re})\right)^{1/2}}, \tag{141}$$

$$\mathrm{Nu} = \frac{\mathrm{Ra}^{1/2}\mathrm{Pr}^{-1/4}}{\left(\ln(\mathrm{Re})\right)^{3/2}}, \tag{142}$$

which is the result of Kraichnan. Using equation (76):

$$\frac{\Theta}{\Delta} = \mathrm{Pr}^{-1/2}. \tag{143}$$

9.3. *The observation of Cioni et al.*

During one of the runs of their mercury experiment, Cioni et al. [15] observed a rapid increase of the Nusselt number on a limited range of Rayleigh numbers. Their interpretation was a transition between two regimes. However, as shown on the Figure 9, this rapid increase nicely fits with the predicted behavior, equation (109), in a GL case $(\mathrm{IV})_\mathrm{l}$, and intermediate turbulence.

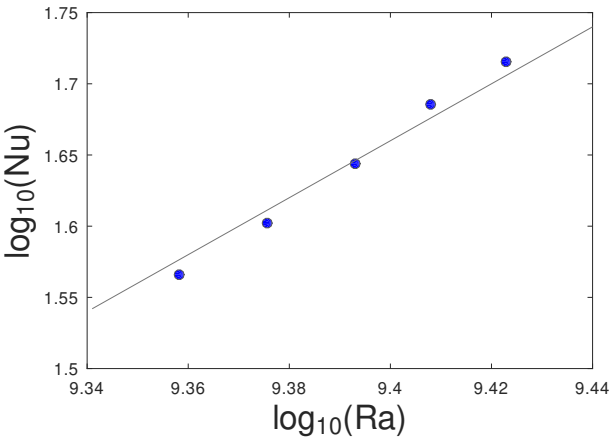

Figure 9. Part of the Cioni et al. results [15], corresponding to their "rapid increase" in Nusselt number, in logarithmic coordinates. The continuous line has a slope 2.

This regime would be much better characterized if Cioni et al. could have measured the Reynolds number or/and the temperature fluctuations simultaneously with these observations. A behavior $\mathrm{Nu} \propto \mathrm{Ra}^2$ is however sufficiently unusual. Moreover, just before this rapid increase, Cioni et al. observed a regime $\mathrm{Nu} \propto \mathrm{Ra}^{1/5}$, which agrees with the low Prandtl number soft turbulence, equation (113). The transition between this regime and the rapid increase of Nu would thus correspond to the transition soft to hard turbulence i.e. the apparition of an inertial cascade. It strongly suggests that the Cioni et al. observation is the only known observed regime of type (IV) in the GL classification.

9.4. *The observation of Chavanne et al.*

Except the Cioni et al. observation discussed above, Chavanne et al. [10] were the first to observe a logarithmic slope μ of Nu versus Ra larger than 1/3. As a tentative interpretation, they assimilated this regime with the Kraichnan regime. However, the observed μ was smaller than 1/2, which

could be attributed to the logarithmic corrections. Later, other authors [35] observed a transition toward a regime with a similar value for μ, larger than 1/3 but smaller than 1/2, while at much higher Rayleigh number.

Indeed, a logarithmic correction is hardly distinguishable from a power law with a small exponent, and even the power law observed on Figure 6 for the second regime could dissimulate a logarithmic correction. Let us however look at equations (124) and (140). They both give Nu as the product of a function of Re and a power of Pr. As ln(Re) mimics a power law, the behavior of the different functions of Re should be close. For the final regime of Chavanne et al., the exponent of Re, $1/(2-\alpha) \simeq 0.81$, and $\mathrm{Nu}/\mathrm{Re}^{0.81}$ should be poorly dependent on Re at constant Pr.

We then select the data for which $3 \cdot 10^5 < \mathrm{Re} < 6 \cdot 10^5$, and plot:

$$\frac{\mathrm{Nu}}{\mathrm{Re}^{0.81}\mathrm{Pr}^{1/2}} \tag{144}$$

versus the Prandtl number, in logarithmic coordinates (see Figure 10). It would give a constant value if the original result of Kraichnan is the good candidate. It would give an ascending slope:

$$\frac{2}{3(2-\alpha)} - \frac{1}{2} \simeq 0.042 \tag{145}$$

in the Blasius case. The results seem to favor the last case.

Does the more recent results [35] correspond to the Blasius or the logarithmic case? It can only be decided through a similar test, involving a large range of Prandtl numbers.

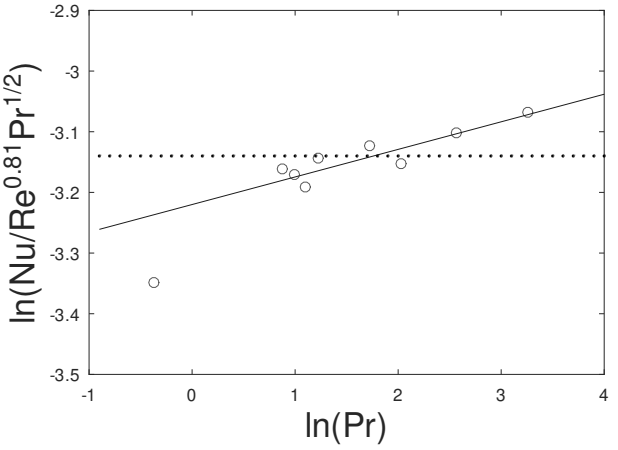

Figure 10. Dependence of the Nusselt number at "constant" Reynolds number ($3 \cdot 10^5 < \mathrm{Re} < 6 \cdot 10^5$), for the Chavanne et al. results [10]. The constant dotted line corresponds to the Kraichnan [25] solution. The continuous line corresponds to the Blasius boundary layer, with $\alpha = 0.77$ (see text).

9.5. *The Shishkina and Lohse model*

During the completion of this work, Shishkina and Lohse [33] published a work which aims at clarifying the "ultimate regimes". They made a great step in this direction, being particularly careful to be consistent with previous [6] and new [34] exact heat transfer upper bounds. They distinguished four regimes, which they called $(\mathrm{IV})'_{\mathrm{l}}$ and $(\mathrm{II})'_{\mathrm{l}}$ for low Prandtl numbers, $(\mathrm{IV})'_{\mathrm{u}}$ and $(\mathrm{III})'_{\infty}$ for large ones.

While our paper is mainly concerned with the structure of the boundary layer, we also treated the bulk for completeness, and the relation between their results and ours is thus important to set. Let us begin with their regimes $(\mathrm{IV})'_\mathrm{l}$ and $(\mathrm{IV})'_\mathrm{u}$. These regimes are dominated by the bulk thermal dissipation, and by the viscous dissipation in a logarithmic boundary layer. As a minor point, and while it is difficult to contradict one of the co-authors of the classification, we tend to consider that, logarithmic or not, a boundary layer is a boundary layer, and the classification would better be $(\mathrm{III})'_\mathrm{l}$ and $(\mathrm{III})'_\mathrm{u}$. We are not in a channel flow, where the logarithmic boundary layer can invade the whole flow, and the exchange of momentum can occur between ascending plumes and descending ones, not only with the walls. This is indeed the case for convection in a vertical channel [36–38]. We expect this is so at extreme Rayleigh numbers, as the non dimensional bulk viscous dissipation, equation (77) grows more rapidly with Re than the logarithmic boundary layer one, equation (68).

Our approach is different from the Shishkina and Lohse [33] one. While our calculus is based on the exact relations concerning viscous and thermal dissipations (equations (12) and (13)), they prefer to modelize the turbulent velocity and heat diffusivities. Using a rather obscure hypothesis (between their equations (11) and (12)), they distinguish between low and large Prandtl numbers.

For low Prandtl numbers, we agree with Shishkina and Lohse [33] on the viscous dissipation in the logarithmic boundary layer:

$$\mathrm{Ra}\,\mathrm{Nu} = \frac{\mathrm{Re}^3\mathrm{Pr}^2}{(\ln \mathrm{Re})^2}, \tag{146}$$

which is our equation (68) and their equation (16) with $\zeta = 0$. For solving in Nu and Re, we use equations (13) and (99):

$$\frac{U\Theta^2}{H} = \kappa\left(\frac{\Delta}{H}\right)^2 \frac{UH}{\nu}\frac{\nu}{\kappa}\frac{\Theta^2}{\Delta^2} = \kappa\left(\frac{\Delta}{H}\right)^2 \mathrm{Nu}, \tag{147}$$

and the evaluation of Θ/Δ with a logarithmic boundary layer, equation (76):

$$\frac{\Theta}{\Delta} = \frac{\mathrm{Nu}(\ln \mathrm{Re})}{\mathrm{Re}\,\mathrm{Pr}}. \tag{148}$$

It results in:

$$\mathrm{Re} = \mathrm{Ra}^{1/2}\mathrm{Pr}^{-1/2}, \tag{149}$$

$$\mathrm{Nu} = \frac{\mathrm{Ra}^{1/2}\mathrm{Pr}^{1/2}}{(\ln \mathrm{Re})^2}, \tag{150}$$

in perfect agreement with Shishkina and Lohse [33].

Things are different for large Prandtl numbers. We consider that the viscous dissipation is not affected by the Prandtl number, and remain with our equation (146). Their approach yields Shishkina and Lohse to introduce an additional Pr^{-1} factor:

$$\mathrm{Ra}\,\mathrm{Nu} = \frac{\mathrm{Re}^3\mathrm{Pr}}{(\ln \mathrm{Re})^2}. \tag{151}$$

It would mean that the viscous dissipation, out of the logarithmic correction, would not only depend on velocity and dimension of the flow, but also on the Prandtl number. This again seems in contradiction with the vertical channel convection [36–38].

As for us, we keep the previous equation (146). The thermal bulk dissipation, as discussed in Section 8.2.5, is dominated by the boundary layer:

$$\mathrm{Nu} = \frac{H}{\delta} = \frac{\mathrm{Re}\,\mathrm{Pr}^{1/3}}{\ln(\mathrm{Re})}. \tag{152}$$

Using equations (152) and (146), we obtain:

$$\mathrm{Re} = \mathrm{Ra}^{1/2}\mathrm{Pr}^{-5/6}(\ln \mathrm{Re})^{1/2}, \tag{153}$$

$$\mathrm{Nu} = \frac{\mathrm{Ra}^{1/2}\mathrm{Pr}^{-1/2}}{(\ln \mathrm{Re})^{1/2}}. \tag{154}$$

It differs from the predictions of Shishkina and Lohse [33]:

$$\mathrm{Re} = \mathrm{Ra}^{1/2}\mathrm{Pr}^{-1/2}, \tag{155}$$

$$\mathrm{Nu} = \frac{\mathrm{Ra}^{1/2}\mathrm{Pr}^{-1/2}}{(\ln \mathrm{Re})^{2}}, \tag{156}$$

both our predictions and theirs being consistent with the Doering and Constantin [6], and Choffrut et al. [34] bounds.

For very high Prandtl numbers ($\mathrm{Pr} > \mathrm{Ra}^{1/3}$), we agree with Shishkina and Lohse that there might be a transition toward $\mathrm{Nu} = \mathrm{Ra}^{1/3}$. Indeed, the above predictions, equations (154) would imply $\mathrm{Nu} < \mathrm{Ra}^{1/3}$, i.e. a thermal boundary layer Rayleigh number, $\mathrm{Ra}/\mathrm{Nu}^3$ indefinitely growing when Ra grows, yielding to its instability.

However, as far as $\mathrm{Pr} < \mathrm{Ra}^{2/3}$, the Reynolds number remains high. Neglecting the logarithmic corrections, equation (77) holds:

$$\mathrm{Ra}\,\mathrm{Nu} = \mathrm{Re}^3\mathrm{Pr}^2 = \mathrm{Ra}^{4/3}. \tag{157}$$

It gives:

$$\mathrm{Re} = \mathrm{Ra}^{4/9}\mathrm{Pr}^{-2/3}, \tag{158}$$

$$\mathrm{Nu} = \mathrm{Ra}^{1/3}. \tag{159}$$

Note that both our scalings and the SL ones ensure the continuity of Nu and Re on the line $\mathrm{Pr} = \mathrm{Ra}^{1/3}$.

For very low Prandtl numbers, Shishkina and Lohse [33] estimate that a transition must occur from the regime $(\mathrm{IV})'_{\mathrm{l}}$ to a regime they call $(\mathrm{II})'_{\mathrm{l}}$, along a line $\mathrm{Ra}\,\mathrm{Pr} = \mathrm{cst}$. They justify this transition in the following term:

> While moving along this line for an increasing Ra and $\mathrm{Pr} \propto \mathrm{Ra}^{-1}$, the Nusselt number remains constant, and any steeper transition slope from regime $(\mathrm{IV})'_{\mathrm{l}}$ would imply an unphysical limit $\mathrm{Nu} \to 0$ along that line.

But the same is true for the scaling they propose: $\mathrm{Nu} \propto (\mathrm{Ra}\,\mathrm{Pr})^{1/5}$. Indeed, they erroneously attribute to Nu the scaling of $(\mathrm{Nu} - 1)$, as we show in the Section 8.2.2.

Table 5 compares our scalings to the SL ones, neglecting the logarithmic corrections.

10. Conclusion

Let us first conclude on the comparison between this work and the results of Shishkina and Lohse [33]. For moderately low Prandtl numbers (regime $(\mathrm{IV})'_{\mathrm{l}}$), we perfectly agree, except that, in our opinion, the really "ultimate" regime is free of logarithmic corrections. For extremely low Prandtl numbers (regime $(\mathrm{II})'_{\mathrm{l}}$), they erroneously attribute to Nu the scaling of $(\mathrm{Nu} - 1)$, but we think this is a misprint due to a lack of attention.

For high Prandtl numbers (regimes $(\mathrm{IV})'_{\mathrm{u}}$ and $(\mathrm{III})'_{\mathrm{u}}$), we disagree. Both our scaling and theirs fit the Constantin–Doering [6] and Choffrut et al. [34] bounds, and both propose a continuous transition, for Nu and Re, on the line $\mathrm{Pr} = \mathrm{Ra}^{1/3}$. Nevertheless, the scalings proposed by Shishkina and Lohse [33] do not agree with the common knowledge on turbulence: their turbulent viscous dissipation is sensitive to the Prandtl number.

Table 5. Comparison between Shishkina and Lohse [33] scalings and ours for ultimate regimes.

	Present work	**Shishkina and Lohse [33]**
$\mathrm{Pr} < \mathrm{Ra}^{-1}$	$\mathrm{Re} = \mathrm{Ra}^{2/5}\mathrm{Pr}^{-3/5}$ $(\mathrm{Nu}-1) = \mathrm{Ra}^{1/5}\mathrm{Pr}^{1/5}$	$\mathrm{Re} = \mathrm{Ra}^{2/5}\mathrm{Pr}^{-3/5}$ $\mathrm{Nu} = \mathrm{Ra}^{1/5}\mathrm{Pr}^{1/5}$
$\mathrm{Ra}^{-1} < \mathrm{Pr} < 1$	$\mathrm{Re} = \mathrm{Ra}^{1/2}\mathrm{Pr}^{-1/2}$ $\mathrm{Nu} = \mathrm{Ra}^{1/2}\mathrm{Pr}^{1/2}$	$\mathrm{Re} = \mathrm{Ra}^{1/2}\mathrm{Pr}^{-1/2}$ $\mathrm{Nu} = \mathrm{Ra}^{1/2}\mathrm{Pr}^{1/2}$
$1 < \mathrm{Pr} < \mathrm{Ra}^{1/3}$	$\mathrm{Re} = \mathrm{Ra}^{1/2}\mathrm{Pr}^{-5/6}$ $\mathrm{Nu} = \mathrm{Ra}^{1/2}\mathrm{Pr}^{-1/2}$	$\mathrm{Re} = \mathrm{Ra}^{1/2}\mathrm{Pr}^{-1/2}$ $\mathrm{Nu} = \mathrm{Ra}^{1/2}\mathrm{Pr}^{-1/2}$
$\mathrm{Ra}^{1/3} < \mathrm{Pr} < \mathrm{Ra}^{2/3}$	$\mathrm{Re} = \mathrm{Ra}^{4/9}\mathrm{Pr}^{-2/3}$ $\mathrm{Nu} = \mathrm{Ra}^{1/3}$	$\mathrm{Re} = \mathrm{Ra}^{2/3}\mathrm{Pr}^{-1}$ $\mathrm{Nu} = \mathrm{Ra}^{1/3}$

Let us give a further argument against the unusual viscous dissipation proposed by Shishkina and Lohse (equation (151)). The free fall velocity of plumes of temperature $\Theta = \Delta\mathrm{Nu}/\mathrm{RePr}$ is $\sqrt{g\beta\Theta H}$, and the corresponding Reynolds number $\mathrm{Re}_{\mathrm{ff}}$ is given by:

$$\mathrm{Re}_{\mathrm{ff}}^2 = \frac{g\beta\Theta H}{\nu^2}H^2 = \frac{\mathrm{Ra}}{\mathrm{Pr}}\frac{\mathrm{Nu}}{\mathrm{RePr}}. \tag{160}$$

Thus, following the Shishkina and Lohse formula, equation (151):

$$\mathrm{Re}_{\mathrm{ff}}^2 = \frac{\mathrm{RaNu}}{\mathrm{RePr}^2} = \frac{\mathrm{Re}^2}{(\ln\mathrm{Re})^2\mathrm{Pr}}, \tag{161}$$

which means that the free fall velocity of the plumes is smaller than the typical velocity of the flow. Our scalings avoid this drawback, but are deeply inspired by their study.

However, the present paper is mainly concerned with the structure of the boundary layer, and its consequences on the dependence of Nusselt and Reynolds numbers on Rayleigh and Prandtl numbers. We succeed in taking into account an often made observation of plumes on the plates, and gave a precise interpretation of Puthenveettil et al. [28] measurements of the total length of plumes per unit area. We show how this total length, or equivalently the distance between plumes, can be related to the observed Nu and Re numbers. The relation between this distance between plumes and the Nusselt number is demonstrated both experimentally and theoretically. The theoretical model we used assumes that the heat flux can be correctly estimated through the product of typical velocity and typical temperature fluctuation. A critical verification of this hypothesis showed us that it is not always the case.

Thus, according to the present work, the various Rayleigh–Bénard convection regimes can be separated in two kinds:

- The unscaling ones. Either because of a transition between two scaling regimes, or due to a special organization of the flow to be elucidated, the cross-correlation coefficient between velocity and temperature cannot be considered as constant. A fundamental hypothesis of many of the proposed models then fails. One can then only rely to the GL theory [7]. Even if their estimation of the boundary layer viscous dissipation appears as too crude, the more elaborated evaluations, like equation (57), are always intermediate between the crude estimation and the bulk dissipation. Thus, estimating the total dissipation as a pondered mean of these two extremes should correctly capture the physics.
- The scaling ones. Then, the cross-correlation coefficient between velocity and temperature can be considered as constant, and a deeper analysis can be performed. It reveals

that different regimes are possible, even for the same Rayleigh number Ra, Prandtl number Pr, and aspect ratio Γ. It also reveals that the evolution of the viscous boundary layer proceeds through a succession of steps toward the turbulent state, rather than through an abrupt and single transition.

One could wonder why we mainly used relatively old experimental results, while more recent, often more precise works exist [35,39,40], including numerical ones [41,42]. The reason is that these works do not provide simultaneous measurements of Nu, Re and Θ. Different regimes have been observed, at the same Rayleigh and Prandtl numbers, even in the same cell. So, simultaneous measurements are essentials. Except in very special cases, as the rapid increase observed by Cioni et al. [15], the behavior of the Nusselt number alone cannot allow to conclude.

The numerical works have the advantage to give access to all the possible measurements. However, for obvious reasons, they hardly give dense series in the Ra, Pr plane. As different regimes rapidly succeed each other, isolated measurements again cannot allow to conclude.

Let us enumerate some aspects of Rayleigh–Bénard convection on which our study gives a new point of view:

- Several studies on two dimensional (2D) Rayleigh–Bénard convection have pointed the remarkable similitude with three dimensions (3D). Indeed, up to the Soft Turbulence included, there are no real differences between 2D and 3D. Only in the Hard Turbulence regime, the energy or enstrophy cascades are dramatically different in 2D and in 3D. In particular, equations (12) and (13) are valid in 2D. Moreover, the influence of the energy cascade only appears in the bulk thermal dissipation, which never dominates in the large Prandtl numbers ultimate regimes. It suggests that a difference between 2D and 3D can only occur at low Prandtl numbers.
- Sharp transitions in the cell behavior can result either from a transition in the bulk (as the transition soft turbulence to hard turbulence) or from a change in the structure of the boundary layer. The latter is not limited to the laminar to turbulent transition. Successive changes in the α value are steps in the evolution from laminar to turbulent. This is exactly the conclusion of Gauthier et al. [43] about the Chavanne observation. They observe that, after the transition, the spectrum of plate temperature fluctuations extends to much higher frequencies, which is coherent with a much smaller development length h.
- Temperature fluctuations measurements are generally easier and more reliable than velocity measurements. Assuming the constancy of the cross-correlation coefficient between vertical velocity and temperature (an assumption implicitly made in several models) gives indirectly access to the Reynolds number through temperature measurements. We urge all experimentalists to include these temperature fluctuations in their data.

Acknowledgments

The authors are thankful to Marc Moulin and his team at the mechanical workshop for the design and machining of the experimental apparatus. We thank Vera Musilová, Michal Macek and Pavel Urban for sharing their data table with us.

Declaration of interests

The authors do not work for, advise, own shares in, or receive funds from any organization that could benefit from this article, and have declared no affiliations other than their research organizations.

References

[1] G. I. Barenblatt, *Scaling, self-similarity, and intermediate asymptotics*, Cambridge Texts in Applied Mathematics, Cambridge University Press, 1996, xxii+386 pages.

[2] D. Lohse and K.-Q. Xia, "Small-scale properties of turbulent Rayleigh–Bénard convection", *Annu. Rev. Fluid Mech.* **42** (2010), pp. 335–364.

[3] F. Chillà and J. Schumacher, "New perspectives in turbulent Rayleigh–Bénard convection", *Eur. Phys. J. E* **35** (2012), pp. 1–25.

[4] G. Ahlers, S. Grossmann and D. Lohse, "Heat transfer and large scale dynamics in turbulent Rayleigh–Bénard convection", *Rev. Mod. Phys.* **81** (2009), article no. 503.

[5] D. Lohse and O. Shishkina, "Ultimate Rayleigh–Bénard turbulence", *Rev. Mod. Phys.* **96** (2024), article no. 035001.

[6] C. R. Doering and P. Constantin, "Variational bounds on energy dissipation in incompressible flows. III. Convection", *Phys. Rev. E* **53** (1996), article no. 5957.

[7] S. Grossmann and D. Lohse, "Scaling in thermal convection: a unifying theory", *J. Fluid Mech.* **407** (2000), pp. 27–56.

[8] R. J. A. M. Stevens, E. P. van der Poel, S. Grossmann and D. Lohse, "The unifying theory of scaling in thermal convection: the updated prefactors", *J. Fluid Mech.* **730** (2013), pp. 295–308.

[9] M. V. R. Malkus, "The heat transport and spectrum of thermal turbulence", *Proc. R. Soc. Lond., Ser. A* **225** (1954), no. 1161, pp. 196–212.

[10] X. Chavanne, F. Chillà, B. Chabaud, B. Castaing and B. Hébral, "Turbulent Rayleigh–Bénard convection in gaseous and liquid He", *Phys. Fluids* **13** (2001), no. 5, pp. 1300–1320.

[11] P. E. Dimotakis, "The mixing transition in turbulent flows", *J. Fluid Mech.* **409** (2000), pp. 69–98.

[12] B. Castaing, E. Rusaouën, J. Salort and F. Chillà, "Turbulent heat transport regimes in a channel", *Phys. Rev. Fluids* **2** (2017), article no. 062801.

[13] B. Castaing et al., "Scaling of hard thermal turbulence in Rayleigh–Bénard convection", *J. Fluid Mech.* **204** (1989), pp. 1–30.

[14] X. Z. Wu, *Along a road to developed turbulence: Free thermal convection in low temperature helium gas*, PhD thesis, University of Chicago (USA), 1991.

[15] S. Cioni, S. Ciliberto and J. Sommeria, "Strongly turbulent Rayleigh–Bénard convection in mercury: comparison with results at moderate Prandtl number", *J. Fluid Mech.* **335** (1997), pp. 111–140.

[16] P.-E. Roche, B. Castaing, B. Chabaud and B. Hébral, "Prandtl and Rayleigh numbers dependences in Rayleigh–Bénard convection", *Eur. Phys. Lett.* **58** (2002), no. 5, article no. 693.

[17] F. Chillà, M. Rastello, S. Chaumat and B. Castaing, "Long relaxation times and tilt sensitivity in Rayleigh–Bénard turbulence", *Eur. Phys. J. B, Condens. Matter Complex Syst.* **40** (2004), pp. 223–227.

[18] B. Dubrulle, "Scaling in large Prandtl number turbulent thermal convection", *Eur. Phys. J. B, Condens. Matter Complex Syst.* **28** (2002), pp. 361–367.

[19] P.-E. Roche, B. Castaing, B. Chabaud, B. Hébral and J. Sommeria, "Side wall effects in Rayleigh–Bénard experiments", *Eur. Phys. J. B, Condens. Matter Complex Syst.* **24** (2001), pp. 405–408.

[20] G. Ahlers, "Effect of sidewall conductance on heat-transport measurements for turbulent Rayleigh–Bénard convection", *Phys. Rev. E* **63** (2000), article no. 015303 (4 pages).

[21] V. Musilovà, T. Kràlík, M. La Mantia, M. Macek, P. Urban and L. Skrbek, "Reynolds number scaling in cryogenic turbulent Rayleigh–Bénard convection in a cylindrical aspect ratio one cell", *J. Fluid Mech.* **832** (2017), pp. 721–744.

[22] M. Belkadi, L. Guislain, A. Sergent, B. Podvin, F. Chillà and J. Salort, "Experimental and numerical shadowgraph in turbulent Rayleigh–Bénard convection with a rough boundary: investigation of plumes", *J. Fluid Mech.* **895** (2020), article no. A7.

[23] M. Belkadi, A. Sergent, Y. Fraigneau and B. Podvin, "On the role of roughness valleys in turbulent Rayleigh–Bénard convection", *J. Fluid Mech.* **923** (2021), article no. A6 (22 pages).

[24] E. S. C. Ching, "Heat flux and shear rate in turbulent convection", *Phys. Rev. E* **55** (1997), pp. 1189–1192.

[25] R. H. Kraichnan, "Turbulent thermal convection at arbitrary Prandtl number", *Phys. Fluids* **5** (1962), no. 11, pp. 1374–1389.

[26] L. D. Landau and E. M. Lifchitz, *Physique théorique. Tome VI: Mécanique des fluides*, Éditions Mir, 1971, 669 pages.

[27] R. Verzicco and R. Camussi, "Prandtl number effects in convective turbulence", *J. Fluid Mech.* **383** (1999), pp. 55–73.

[28] B. A. Puthenveettil, G. S. Gunasegarane, Y. K. Agrawal, D. Schmeling, J. Bosbach and J. H. Arakeri, "Length of near-wall plumes in turbulent convection", *J. Fluid Mech.* **685** (2011), pp. 335–364.

[29] G. Zocchi, E. Moses and A. Libchaber, "Coherent structures in turbulent convection, an experimental study", *Phys. A: Stat. Mech. Appl.* **166** (1990), no. 3, pp. 387–407.

[30] É. Guyon, J.-P. Hulin and L. Petit, *Hydrodynamique physique*, 3rd edition, Savoirs actuels, EDP Sciences, 2012, 724 pages.

[31] G. Ahlers, E. Bodenschatz and X. He, "Logarithmic temperature profiles of turbulent Rayleigh–Bénard convection in the classical and ultimate state for a Prandtl number of 0.8", *J. Fluid Mech.* **758** (2014), pp. 436–467.

[32] U. Frisch, *Turbulence*, Cambridge University Press, 1995, 312 pages.

[33] O. Shishkina and D. Lohse, "Ultimate regime of Rayleigh–Bénard turbulence: subregimes and their scaling relations for the Nusselt vs Rayleigh and Prandtl numbers", *Phys. Rev. Lett.* **133** (2024), article no. 144001 (7 pages).

[34] A. Choffrut, C. Nobili and F. Otto, "Upper bounds on Nusselt number at finite Prandtl number", *J. Differ. Equations* **260** (2016), no. 4, pp. 3860–3880.

[35] X. He, D. P. M. van Gils, E. Bodenschatz and G. Ahlers, "Reynolds numbers and the elliptic approximation near the ultimate state of turbulent Rayleigh–Bénard convection", *New J. Phys.* **17** (2015), article no. 063028 (26 pages).

[36] M. Cholemari and J. H. Arakeri, "Axially homogeneous, zero mean flow buoyancy-driven turbulence in a vertical pipe", *J. Fluid Mech.* **621** (2009), pp. 69–102.

[37] J.-C. Tisserand, M. Creyssels, M. Gibert, B. Castaing and F. Chillà, "Convection in a vertical channel", *New J. Phys.* **12** (2010), article no. 075024 (21 pages).

[38] E. Calzavarini, D. Lohse, F. Toschi and R. Tripiccione, "Rayleigh and Prandtl number scaling in the bulk of Rayleigh–Bénard turbulence", *Phys. Fluids* **17** (2005), no. 5, article no. 055107.

[39] J. J. Niemela, L. Skrbek, K. R. Sreenivasan and R. J. Donnelly, "Turbulent convection at very high Rayleigh numbers", *Nature* **404** (2000), pp. 837–840.

[40] P.-E. Roche, F. Gauthier, R. Kaiser and J. Salort, "On the triggering of the Ultimate Regime of convection", *New J. Phys.* **12** (2010), article no. 085014 (26 pages).

[41] R. J. A. M. Stevens, D. Lohse and R. Verzicco, "Prandtl and Rayleigh number dependence of heat transport in high Rayleigh number thermal convection", *J. Fluid Mech.* **688** (2011), pp. 31–43.

[42] J. Bailon-Cuba, M. S. Emran and J. Schumacher, "Aspect ratio dependence of heat transfer and large-scale flow in turbulent convection", *J. Fluid Mech.* **655** (2010), pp. 152–173.

[43] F. Gauthier and P.-E. Roche, "Evidence of a boundary layer instability at very high Rayleigh number", *Eur. Phys. Lett.* **83** (2008), no. 2, article no. 24005.